

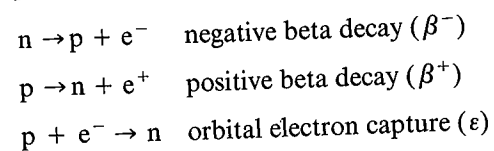
BETA DECAY

The emission of ordinary negative electrons from the nucleus was among the earliest observed radioactive decay phenomena. The inverse process, capture by a nucleus of an electron from its atomic orbital, was not observed until 1938 when Alvarez detected the characteristic X rays emitted in the filling of the vacancy left by the captured electron. The Joliot-Curies in 1934 first observed the related process of positive electron (positron) emission in radioactive decay, only two years after the positron had been discovered in cosmic rays. These three nuclear processes are closely related and are grouped under the common name *beta* (β) decay.

The most basic β decay process is the conversion of a proton to a neutron or of a neutron into a proton. In a nucleus, β decay changes both Z and N by one unit: $Z \rightarrow Z \pm 1$, $N \rightarrow N \mp 1$ so that $A = Z + N$ remains constant. Thus β decay provides a convenient way for an unstable nucleus to "slide down" the mass parabola (Figure 3.18, for example) of constant A and to approach the stable isobar.

In contrast with α decay, progress in understanding β decay has been achieved at an extremely slow pace, and often the experimental results have created new puzzles that challenged existing theories. Just as Rutherford's early experiments showed α particles to be identical with ${}^4\text{He}$ nuclei, other early experiments showed the negative β particles to have the same electric charge and charge-to-mass ratio as ordinary electrons. In Section 1.2, we discussed the evidence against the presence of electrons as nuclear constituents, and so we must regard the β decay process as "creating" an electron from the available decay energy at the instant of decay; this electron is then immediately ejected from the nucleus. This situation contrasts with α decay, in which the α particle may be regarded as having a previous existence in the nucleus.

The basic decay processes are thus:



These processes are not complete, for there is yet another particle (a neutrino or antineutrino) involved in each. The latter two processes occur only for protons

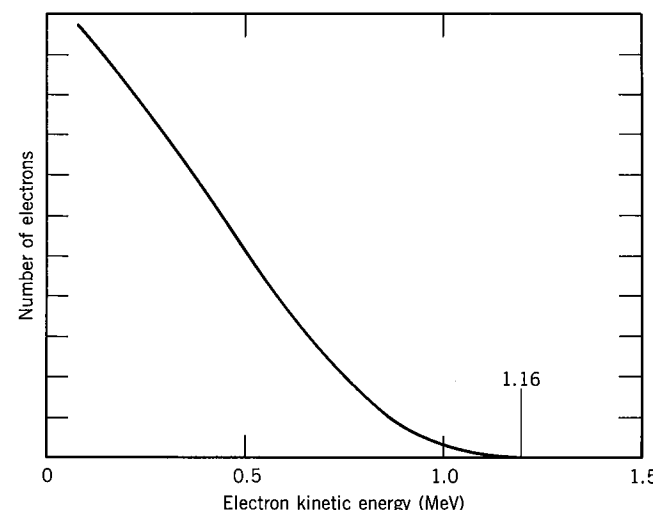


Figure 9.1 The continuous electron distribution from the β decay of ${}^{210}\text{Bi}$ (also called RaE in the literature).

bound in nuclei; they are energetically forbidden for free protons or for protons in hydrogen atoms.

9.1 ENERGY RELEASE IN β DECAY

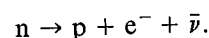
The continuous energy distribution of the β -decay electrons was a confusing experimental result in the 1920s. Alpha particles are emitted with sharp, well-defined energies, equal to the difference in mass energy between the initial and final states (less the small recoil corrections); all α decays connecting the same initial and final states have exactly the same kinetic energies. Beta particles have a continuous distribution of energies, from zero up to an upper limit (the endpoint energy) which is equal to the energy difference between the initial and final states. If β decay were, like α decay, a two-body process, we would expect all of the β particles to have a unique energy, but virtually all of the emitted particles have a smaller energy. For instance, we might expect on the basis of nuclear mass differences that the β particles from ${}^{210}\text{Bi}$ would be emitted with a kinetic energy of 1.16 MeV, yet we find a continuous distribution from 0 up to 1.16 MeV (Figure 9.1).

An early attempt to account for this "missing" energy hypothesized that the β 's are actually emitted with 1.16 MeV of kinetic energy, but lose energy, such as by collisions with atomic electrons, before they reach the detection system. Such a possibility was eliminated by very precise calorimetric experiments that confined a β source and measured its decay energy by the heating effect. If a portion of the energy were transferred to the atomic electrons, a corresponding rise in temperature should be observed. These experiments showed that the shape of the spectrum shown in Figure 9.1 is a characteristic of the decay electrons themselves and not a result of any subsequent interactions.

To account for this energy release, Pauli in 1931 proposed that there was emitted in the decay process a second particle, later named by Fermi the

neutrino. The neutrino carries the “missing” energy and, because it is highly penetrating radiation, it is not stopped within the calorimeter, thus accounting for the failure of those experiments to record its energy. Conservation of electric charge requires the neutrino to be electrically neutral, and angular momentum conservation and statistical considerations in the decay process require the neutrino to have (like the electron) a spin of $\frac{1}{2}$. Experiment shows that there are in fact two different kinds of neutrinos emitted in β decay (and yet other varieties emitted in other decay processes; see Chapter 18). These are called the *neutrino* and the *antineutrino* and indicated by ν and $\bar{\nu}$. It is the antineutrino which is emitted in β^- decay and the neutrino which is emitted in β^+ decay and electron capture. In discussing β decay, the term “neutrino” is often used to refer to both neutrinos and antineutrinos, although it is of course necessary to distinguish between them in writing decay processes; the same is true for “electron.”

To demonstrate β -decay energetics we first consider the decay of the free neutron (which occurs with a half-life of about 10 min),



As we did in the case of α decay, we define the Q value to be the difference between the initial and final *nuclear* mass energies.

$$Q = (m_n - m_p - m_e - m_{\bar{\nu}})c^2 \quad (9.1)$$

and for decays of neutrons at rest,

$$Q = T_p + T_e + T_{\bar{\nu}} \quad (9.2)$$

For the moment we will ignore the proton recoil kinetic energy T_p , which amounts to only 0.3 keV. The antineutrino and electron will then share the decay energy, which accounts for the continuous electron spectrum. The maximum-energy electrons correspond to minimum-energy antineutrinos, and when the antineutrinos have vanishingly small energies, $Q \approx (T_e)_{\max}$. The measured maximum energy of the electrons is 0.782 ± 0.013 MeV. Using the measured neutron, electron, and proton masses, we can compute the Q value:

$$\begin{aligned} Q &= m_n c^2 - m_p c^2 - m_e c^2 - m_{\bar{\nu}} c^2 \\ &= 939.573 \text{ MeV} - 938.280 \text{ MeV} - 0.511 \text{ MeV} - m_{\bar{\nu}} c^2 \\ &= 0.782 \text{ MeV} - m_{\bar{\nu}} c^2 \end{aligned}$$

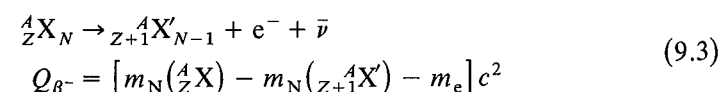
Thus to within the precision of the measured maximum energy (about 13 keV) we may regard the antineutrino as massless. Other experiments provide more stringent upper limits, as we discuss in Section 9.6, and for the present discussion we take the masses of the neutrino and antineutrino to be identically zero.

Conservation of linear momentum can be used to identify β decay as a three-body process, but this requires measuring the momentum of the recoiling nucleus in coincidence with the momentum of the electron. These experiments are difficult, for the low-energy nucleus ($T \lesssim \text{keV}$) is easily scattered, but they have been done in a few cases, from which it can be deduced that the vector sum of the linear momenta of the electron and the recoiling nucleus is consistent with an unobserved third particle carrying the “missing” energy and having a rest mass of zero or nearly zero. Whatever its mass might be, the existence of the

additional particle is absolutely required by these experiments, for the momenta of the electron and nucleus certainly do not sum to zero, as they would in a two-body decay.

Because the neutrino is massless, it moves with the speed of light and its total relativistic energy E_{ν} is the same as its kinetic energy; we will use E_{ν} to represent neutrino energies. (A review of the concepts and formulas of relativistic kinematics may be found in Appendix A.) For the electron, we will use both its kinetic energy T_e and its total relativistic energy E_e , which are of course related by $E_e = T_e + m_e c^2$. (Decay energies are typically of order MeV; thus the nonrelativistic approximation $T \ll mc^2$ is certainly not valid for the decay electrons, and we *must* use relativistic kinematics.) The nuclear recoil is of very low energy and can be treated nonrelativistically.

Let's consider a typical negative β -decay process in a nucleus:



where m_N indicates *nuclear* masses. To convert nuclear masses into the tabulated neutral atomic masses, which we denote as $m({}^A X)$, we use

$$m({}^A X)c^2 = m_N({}^A X)c^2 + Zm_e c^2 - \sum_{i=1}^Z B_i \quad (9.4)$$

where B_i represents the binding energy of the i th electron. In terms of atomic masses,

$$\begin{aligned} Q_{\beta^-} &= \{[m({}^A X) - Zm_e] - [m({}^A X') - (Z+1)m_e] - m_e\}c^2 \\ &\quad + \left\{ \sum_{i=1}^Z B_i - \sum_{i=1}^{Z+1} B_i \right\} \end{aligned} \quad (9.5)$$

Notice that the electron masses cancel in this case. Neglecting the differences in electron binding energy, we therefore find

$$Q_{\beta^-} = [m({}^A X) - m({}^A X')]c^2 \quad (9.6)$$

where the masses are neutral atomic masses. The Q value represents the energy shared by the electron and neutrino:

$$Q_{\beta^-} = T_e + E_{\bar{\nu}} \quad (9.7)$$

and it follows that each has its maximum when the other approaches zero:

$$(T_e)_{\max} = (E_{\bar{\nu}})_{\max} = Q_{\beta^-} \quad (9.8)$$

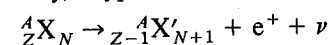
In the case of the ${}^{210}\text{Bi} \rightarrow {}^{210}\text{Po}$ decay, the mass tables give

$$\begin{aligned} Q_{\beta^-} &= [m({}^{210}\text{Bi}) - m({}^{210}\text{Po})]c^2 \\ &= (209.984095 \text{ u} - 209.982848 \text{ u})(931.502 \text{ MeV/u}) \\ &= 1.161 \text{ MeV} \end{aligned}$$

Figure 9.1 showed $(T_e)_{\max} = 1.16$ MeV, in agreement with the value expected from Q_{β^-} . Actually, this is really not an agreement between two independent values. The value of Q_{β^-} is used in this case to *determine* the mass of ${}^{210}\text{Po}$, with

the mass of ^{210}Bi determined from that of ^{209}Bi using neutron capture. Equation 9.6 is used with the measured Q_{β^-} to obtain $m(^A\text{X}')$.

In the case of positron decay, a typical decay process is

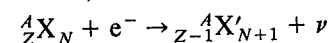


and a calculation similar to the previous one shows

$$Q_{\beta^+} = [m(^A\text{X}) - m(^A\text{X}') - 2m_e]c^2 \quad (9.9)$$

again using atomic masses. Notice that the electron masses *do not* cancel in this case.

For electron-capture processes, such as



the calculation of the Q value must take into account that the atom X' is in an atomic excited state immediately after the capture. That is, if the capture takes place from an inner shell, the K shell for instance, an electronic vacancy in that shell results. The vacancy is quickly filled as electrons from higher shells make downward transitions and emit characteristic X rays. Whether one X ray is emitted or several, the total X-ray energy is equal to the binding energy of the captured electron. Thus the atomic mass of X' immediately after the decay is greater than the mass of X' in its atomic ground state by B_n , the binding energy of the captured n -shell electron ($n = \text{K, L, } \dots$). The Q value is then

$$Q_e = [m(^A\text{X}) - m(^A\text{X}') + B_n]c^2 \quad (9.10)$$

Positive beta decay and electron capture both lead from the initial nucleus ${}^A_Z\text{X}_N$ to the final nucleus ${}^A_{Z-1}\text{X}'_{N+1}$, but note that both may not always be energetically possible (Q must be positive for any decay process). Nuclei for which β^+ decay is energetically possible may also undergo electron capture, but the reverse is not true—it is possible to have $Q > 0$ for electron capture while $Q < 0$ for β^+ decay. The atomic mass energy difference must be at least $2m_e c^2 = 1.022 \text{ MeV}$ to permit β^+ decay.

In positron decay, expressions of the form of Equations 9.7 and 9.8 show that there is a continuous distribution of neutrino energies up to Q_{β^+} (less the usually negligible nuclear recoil). In electron capture, however, the two-body final state results in unique values for the recoil energy and E_ν . Neglecting the recoil, a monoenergetic neutrino with energy Q_e is emitted.

All of the above expressions refer to decays between nuclear ground states. If the final nuclear state X' is an excited state, the Q value must be accordingly

Table 9.1 Typical β -Decay Processes

Decay	Type	Q (MeV)	$t_{1/2}$
$^{23}\text{Ne} \rightarrow ^{23}\text{Na} + e^- + \bar{\nu}$	β^-	4.38	38 s
$^{99}\text{Tc} \rightarrow ^{99}\text{Ru} + e^- + \bar{\nu}$	β^-	0.29	$2.1 \times 10^5 \text{ y}$
$^{25}\text{Al} \rightarrow ^{25}\text{Mg} + e^+ + \nu$	β^+	3.26	7.2 s
$^{124}\text{I} \rightarrow ^{124}\text{Te} + e^+ + \nu$	β^+	2.14	4.2 d
$^{15}\text{O} + e^- \rightarrow ^{15}\text{N} + \nu$	ϵ	2.75	1.22 s
$^{41}\text{Ca} + e^- \rightarrow ^{41}\text{K} + \nu$	ϵ	0.43	$1.0 \times 10^5 \text{ y}$

decreased by the excitation energy of the state:

$$Q_{\text{ex}} = Q_{\text{ground}} - E_{\text{ex}} \quad (9.11)$$

Table 9.1 shows some typical β decay processes, their energy releases, and their half-lives.

9.2 FERMI THEORY OF β DECAY

In our calculation of α -decay half-lives in Chapter 8, we found that the barrier penetration probability was the critical factor in determining the half-life. In negative β decay there is no such barrier to penetrate and even in β^+ decay, it is possible to show from even a rough calculation that the exponential factor in the barrier penetration probability is of order unity. There are other important differences between α and β decay which suggest to us that we must use a completely different approach for the calculation of transition probabilities in β decay: (1) The electron and neutrino do not exist before the decay process, and therefore we must account for the formation of those particles. (2) The electron and neutrino must be treated relativistically. (3) The continuous distribution of electron energies must result from the calculation.

In 1934, Fermi developed a successful theory of β decay based on Pauli's neutrino hypothesis. The essential features of the decay can be derived from the basic expression for the transition probability caused by an interaction that is weak compared with the interaction that forms the quasi-stationary states. This is certainly true for β decay, in which the characteristic times (the half-lives, typically of order seconds or longer) are far longer than the characteristic nuclear time (10^{-20} s). The result of this calculation, treating the decay-causing interaction as a weak perturbation, is Fermi's Golden Rule, a general result for any transition rate previously given in Equation 2.79:

$$\lambda = \frac{2\pi}{\hbar} |V_{fi}|^2 \rho(E_f) \quad (9.12)$$

The matrix element V_{fi} is the integral of the interaction V between the initial and final quasi-stationary states of the system:

$$V_{fi} = \int \psi_f^* V \psi_i d\mathbf{v} \quad (9.13)$$

The factor $\rho(E_f)$ is the density of final states, which can also be written as dn/dE_f , the number dn of final states in the energy interval dE_f . A given transition is more likely to occur if there is a large number of accessible final states.

Fermi did not know the mathematical form of V for β decay that would have permitted calculations using Equations 9.12 and 9.13. Instead, he considered all possible forms consistent with special relativity, and he showed that V could be replaced with one of five mathematical operators O_X , where the subscript X gives the form of the operator O (that is, its transformation properties): $X = \text{V}$ (vector), A (axial vector), S (scalar), P (pseudoscalar), or T (tensor). Which of these is correct for β decay can be revealed only through experiments that study

the symmetries and the spatial properties of the decay products, and it took 20 years (and several mistaken conclusions) for the correct V-A form to be deduced.

The final state wave function must include not only the nucleus but also the electron and neutrino. For electron capture or neutrino capture, the forms would be similar, but the appropriate wave function would appear in the initial state. For β decay, the interaction matrix element then has the form

$$V_{fi} = g \int [\psi_f^* \varphi_e^* \varphi_\nu^*] O_X \psi_i dv \quad (9.14)$$

where now ψ_f refers only to the final nuclear wave function and φ_e and φ_ν give the wave functions of the electron and neutrino. The quantity in square brackets represents the entire final system after the decay. The value of the constant g determines the strength of the interaction; the electronic charge e plays a similar role in the interaction between an atom and the electromagnetic field.

The density of states factor determines (to lowest order) the shape of the beta energy spectrum. To find the density of states, we need to know the number of final states accessible to the decay products. Let us suppose in the decay that we have an electron (or positron) emitted with momentum p and a neutrino (or antineutrino) with momentum q . We are interested at this point only in the *shape* of the energy spectrum, and thus the directions of p and q are of no interest. If we imagine a coordinate system whose axes are labeled p_x, p_y, p_z , then the locus of the points representing a specific value of $|p| = (p_x^2 + p_y^2 + p_z^2)^{1/2}$ is a sphere of radius $p = |p|$. More specifically, the locus of points representing momenta in the range dp at p is a spherical shell of radius p and thickness dp , thus having volume $4\pi p^2 dp$. If the electron is confined to a box of volume V (this step is taken only for completeness and to permit the wave function to be normalized; the actual volume will cancel from the final result), then the number of final electron states dn_e , corresponding to momenta in the range p to $p + dp$, is

$$dn_e = \frac{4\pi p^2 dp V}{h^3} \quad (9.15)$$

where the factor h^3 is included to make the result a dimensionless pure number.* Similarly, the number of neutrino states is

$$dn_\nu = \frac{4\pi q^2 dq V}{h^3} \quad (9.16)$$

and the number of final states which have simultaneously an electron and a neutrino with the proper momenta is

$$d^2n = dn_e dn_\nu = \frac{(4\pi)^2 V^2 p^2 dp q^2 dq}{h^6} \quad (9.17)$$

*The available spatial and momentum states are counted in six-dimensional (x, y, z, p_x, p_y, p_z) phase space; the unit volume in phase space is h^3 .

The electron and neutrino wave functions have the usual free-particle form, normalized within the volume V :

$$\begin{aligned} \varphi_e(\mathbf{r}) &= \frac{1}{\sqrt{V}} e^{i\mathbf{p} \cdot \mathbf{r}/\hbar} \\ \varphi_\nu(\mathbf{r}) &= \frac{1}{\sqrt{V}} e^{i\mathbf{q} \cdot \mathbf{r}/\hbar} \end{aligned} \quad (9.18)$$

For an electron with 1 MeV kinetic energy, $p = 1.4 \text{ MeV}/c$ and $p/\hbar = 0.007 \text{ fm}^{-1}$. Thus over the nuclear volume, $pr \ll 1$ and we can expand the exponentials, keeping only the first term:

$$\begin{aligned} e^{i\mathbf{p} \cdot \mathbf{r}/\hbar} &= 1 + \frac{i\mathbf{p} \cdot \mathbf{r}}{\hbar} + \dots \cong 1 \\ e^{i\mathbf{q} \cdot \mathbf{r}/\hbar} &= 1 + \frac{i\mathbf{q} \cdot \mathbf{r}}{\hbar} + \dots \cong 1 \end{aligned} \quad (9.19)$$

This approximation is known as the *allowed* approximation.

In this approximation, the only factors that depend on the electron or neutrino energy come from the density of states. Let's assume we are trying to calculate the momentum and energy distributions of the emitted electrons. The partial decay rate for electrons and neutrinos with the proper momenta is

$$d\lambda = \frac{2\pi}{\hbar} g^2 |M_{fi}|^2 (4\pi)^2 \frac{p^2 dp q^2 dq}{h^6} \frac{dE_f}{dE_i} \quad (9.20)$$

where $M_{fi} = \int \psi_f^* O_X \psi_i dv$ is the *nuclear matrix element*. The final energy E_f is just $E_e + E_\nu = E_e + qc$, and so $dq/dE_f = 1/c$ at fixed E_e . As far as the shape of the electron spectrum is concerned, all of the factors in Equation 9.20 that do not involve the momentum (including M_{fi} , which for the present we assume to be independent of p) can be combined into a constant C , and the resulting distribution gives the number of electrons with momentum between p and $p + dp$:

$$N(p) dp = C p^2 q^2 dp \quad (9.21)$$

If Q is the decay energy, then ignoring the negligible nuclear recoil energy,

$$q = \frac{Q - T_e}{c} = \frac{Q - \sqrt{p^2 c^2 + m_e^2 c^4} + m_e c^2}{c} \quad (9.22)$$

and the spectrum shape is given by

$$N(p) = \frac{C}{c^2} p^2 (Q - T_e)^2 \quad (9.23)$$

$$= \frac{C}{c^2} p^2 \left[Q - \sqrt{p^2 c^2 + m_e^2 c^4} + m_e c^2 \right]^2 \quad (9.24)$$

This function vanishes at $p = 0$ and also at the endpoint where $T_e = Q$; its shape is shown in Figure 9.2.

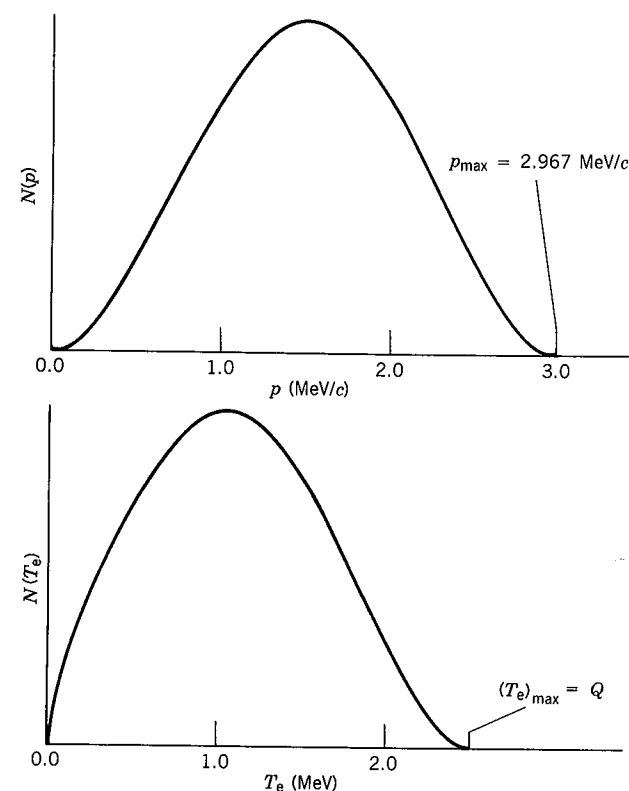


Figure 9.2 Expected electron energy and momentum distributions, from Equations 9.24 and 9.25. These distributions are drawn for $Q = 2.5$ MeV.

More frequently we are interested in the energy spectrum, for electrons with kinetic energy between T_e and $T_e + dT_e$. With $c^2 p dp = (T_e + m_e c^2) dT_e$, we have

$$N(T_e) = \frac{C}{c^5} (T_e^2 + 2T_e m_e c^2)^{1/2} (Q - T_e)^2 (T_e + m_e c^2) \quad (9.25)$$

This distribution, which also vanishes at $T_e = 0$ and at $T_e = Q$, is shown in Figure 9.2.

In Figure 9.3, the β^+ and β^- decays of ^{64}Cu are compared with the predictions of the theory. As you can see, the general shape of Figure 9.2 is evident, but there are systematic differences between theory and experiment. These differences originate with the Coulomb interaction between the β particle and the daughter nucleus. Semiclassically, we can interpret the shapes of the momentum distributions of Figure 9.3 as a Coulomb repulsion of β^+ by the nucleus, giving fewer low-energy positrons, and a Coulomb attraction of β^- , giving more low-energy electrons. From the more correct standpoint of quantum mechanics, we should instead refer to the change in the electron plane wave, Equation 9.19, brought about by the Coulomb potential inside the nucleus. The quantum mechanical calculation of the effect of the nuclear Coulomb field on the electron wave function is beyond the level of this text. It modifies the spectrum by introducing an additional factor, the *Fermi function* $F(Z', p)$ or $F(Z', T_e)$, where Z' is the atomic number of the daughter nucleus. Finally, we must

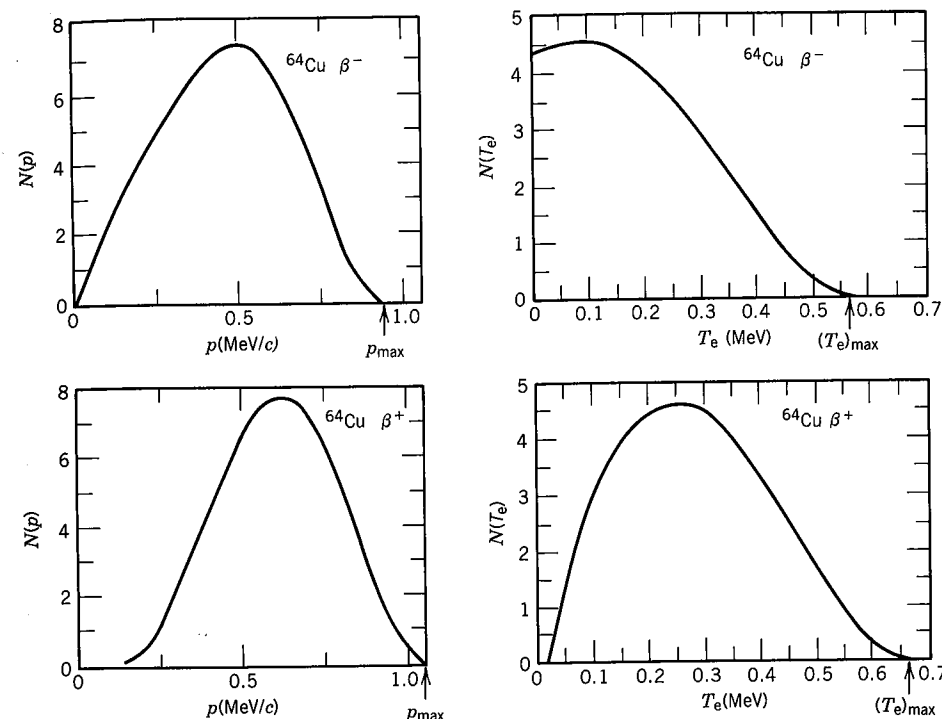


Figure 9.3 Momentum and kinetic energy spectra of electrons and positrons emitted in the decay of ^{64}Cu . Compare with Figure 9.2; the differences arise from the Coulomb interactions with the daughter nucleus. From R. D. Evans, *The Atomic Nucleus* (New York: McGraw-Hill, 1955).

consider the effect of the nuclear matrix element, M_{fi} , which we have up to now assumed not to influence the shape of the spectrum. This approximation (also called the allowed approximation) is often found to be a very good one, but there are some cases in which it is very bad—in fact, there are cases in which M_{fi} vanishes in the allowed approximation, giving no spectrum at all! In such cases, we must take the next terms of the plane wave expansion, Equations 9.19, which introduce yet another momentum dependence. Such cases are called, somewhat incorrectly, *forbidden* decays; these decays are not absolutely forbidden, but as we will learn subsequently, they are less likely to occur than allowed decays and therefore tend to have longer half-lives. The degree to which a transition is forbidden depends on how far we must take the expansion of the plane wave to find a nonvanishing nuclear matrix element. Thus the first term beyond the 1 gives first-forbidden decays, the next term gives second-forbidden, and so on. We will see in Section 9.4 how the angular momentum and parity selection rules restrict the kinds of decay that can occur.

The complete β spectrum then includes three factors:

1. The *statistical factor* $p^2(Q - T_e)^2$, derived from the number of final states accessible to the emitted particles.
2. The *Fermi function* $F(Z', p)$, which accounts for the influence of the nuclear Coulomb field.

3. The nuclear matrix element $|M_{fi}|^2$, which accounts for the effects of particular initial and final nuclear states and which may include an additional electron and neutrino momentum dependence $S(p, q)$ from forbidden terms:

$$N(p) \propto p^2(Q - T_e)^2 F(Z', p) |M_{fi}|^2 S(p, q) \quad (9.26)$$

9.3 THE "CLASSICAL" EXPERIMENTAL TESTS OF THE FERMI THEORY

The Shape of the β Spectrum

In the allowed approximation, we can rewrite Equation 9.26 as

$$(Q - T_e) \propto \sqrt{\frac{N(p)}{p^2 F(Z', p)}} \quad (9.27)$$

and plotting $\sqrt{N(p)/p^2 F(Z', p)}$ against T_e should give a straight line which intercepts the x axis at the decay energy Q . Such a plot is called a *Kurie plot* (sometimes a Fermi plot or a Fermi-Kurie plot). An example of a Kurie plot is shown in Figure 9.4. The linear nature of this plot gives us confidence in the theory as it has been developed, and also gives us a convenient way to determine the decay endpoint energy (and therefore the Q value).

In the case of forbidden decays, the standard Kurie plot does not give a straight line, but we can restore the linearity of the plot if we instead graph $\sqrt{N(p)/p^2 F(Z', p) S(p, q)}$ against T_e , where S is the momentum dependence that results from the higher-order term in the expansion of the plane wave. The function S is known as the *shape factor*; for certain first-forbidden decays, for example, it is simply $p^2 + q^2$.

Including the shape factor gives a linear plot, as Figure 9.5 shows.

The Total Decay Rate

To find the total decay rate, we must integrate Equation 9.20 over all values of the electron momentum p , keeping the neutrino momentum at the value determined by Equation 9.22, which of course also depends on p . Thus, for allowed decays,

$$\lambda = \frac{g^2 |M_{fi}|^2}{2\pi^3 \hbar^7 c^3} \int_0^{p_{\max}} F(Z', p) p^2 (Q - T_e)^2 dp \quad (9.28)$$

The integral will ultimately depend only on Z' and on the maximum electron total energy E_0 (since $cp_{\max} = \sqrt{E_0^2 - m_e^2 c^4}$), and we therefore represent it as

$$f(Z', E_0) = \frac{1}{(m_e c)^3 (m_e c^2)^2} \int_0^{p_{\max}} F(Z', p) p^2 (E_0 - E_e)^2 dp \quad (9.29)$$

where the constants have been included to make f dimensionless. The function $f(Z', E_0)$ is known as the *Fermi integral* and has been tabulated for values of Z' and E_0 .

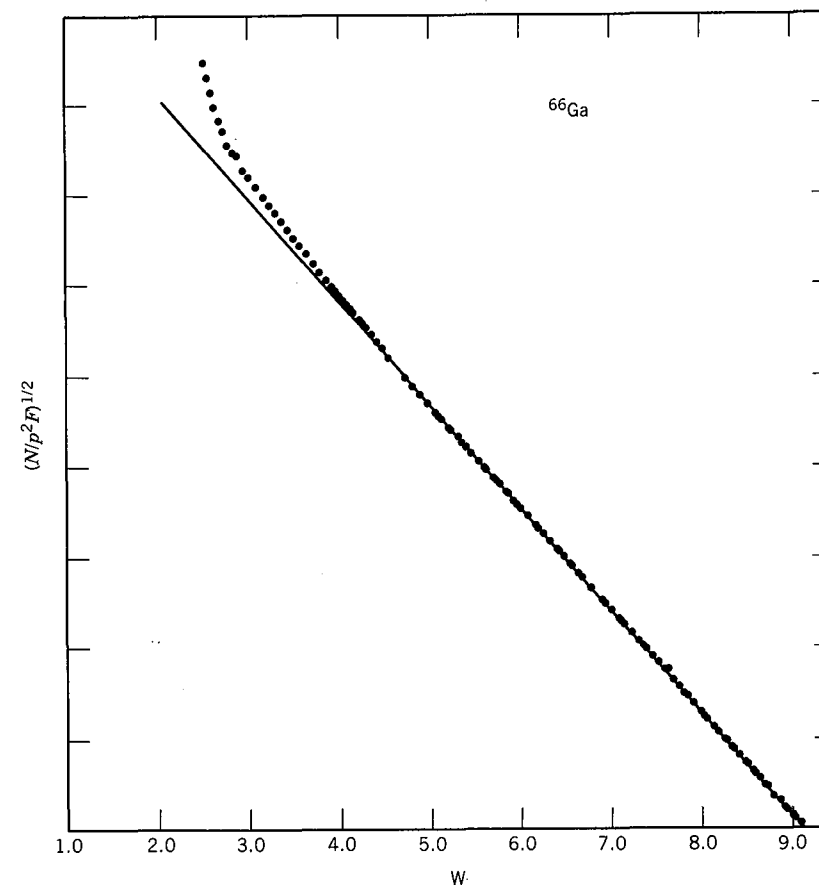


Figure 9.4 Fermi-Kurie plot of allowed $0^+ \rightarrow 0^+$ decay of ^{66}Ga . The horizontal scale is the relativistic total energy ($T_e + m_e c^2$) in units of $m_e c^2$. The deviation from the straight line at low energy arises from the scattering of low-energy electrons within the radioactive source. From D. C. Camp and L. M. Langer, *Phys. Rev.* **129**, 1782 (1963).

With $\lambda = 0.693/t_{1/2}$, we have

$$ft_{1/2} = 0.693 \frac{2\pi^3 \hbar^7}{g^2 m_e^5 c^4 |M_{fi}|^2} \quad (9.30)$$

The quantity on the left side of Equation 9.30 is called the *comparative half-life* or *ft value*. It gives us a way to compare the β -decay probabilities in different nuclei—Equation 9.28 shows that the decay rate depends on Z' and on E_0 , and this dependence is incorporated into f , so that *differences in ft values must be due to differences in the nuclear matrix element* and thus to differences in the nuclear wave function.

As in the case of α decay, there is an enormous range of half-lives in β decay— ft values range from about 10^3 to 10^{20} s. For this reason, what is often quoted is the value of $\log_{10} ft$ (with t given in seconds). The decays with the shortest comparative half-lives ($\log ft \approx 3-4$) are known as *superallowed* decays. Some of

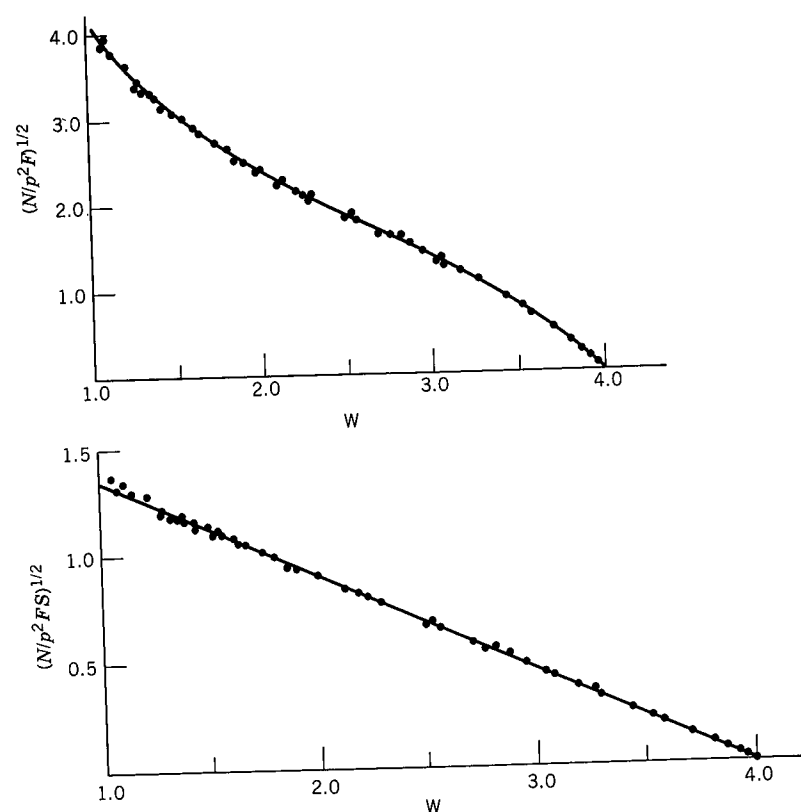


Figure 9.5 Uncorrected Fermi-Kurie plot in the β decay of ^{91}Y (top). The linearity is restored if the shape factor $S(p, q)$ is included; for this type of first-forbidden decay, the shape factor $p^2 + q^2$ gives a linear plot (bottom). Data from L. M. Langer and H. C. Price, *Phys. Rev.* **75**, 1109 (1949).

the superallowed decays have 0^+ initial and final states, in which case the nuclear matrix element can be calculated quite easily: $M_{fi} = \sqrt{2}$. The $\log ft$ values for $0^+ \rightarrow 0^+$ decays should all be identical. Table 9.2 shows the $\log ft$ values of all known $0^+ \rightarrow 0^+$ superallowed transitions, and within experimental error the values appear to be quite constant. Moreover, with $M_{fi} = \sqrt{2}$, we can use Equation 9.30 to find a value of the β -decay strength constant

$$g = 0.88 \times 10^{-4} \text{ MeV} \cdot \text{fm}^3$$

To make this constant more comparable to other fundamental constants, we should express it in a dimensionless form. We can then compare it with dimensionless constants of other interactions (the fine structure constant which characterizes the electromagnetic interaction, for instance). Letting M , L , and T represent, respectively, the dimensions of mass, length, and time, the dimensions of g are $M^1 L^5 T^{-2}$, and no combinations of the fundamental constants \hbar (dimension $M^1 L^2 T^{-1}$) and c (dimension $L^1 T^{-1}$) can be used to convert g into a dimensionless constant. (For instance, $\hbar c^3$ has dimension $M^1 L^5 T^{-5}$, and so $g/\hbar c^3$ has dimension T^3 .) Let us therefore introduce an arbitrary mass m and

Table 9.2 ft Values for $0^+ \rightarrow 0^+$ Superallowed Decays

Decay	ft (s)
$^{10}\text{C} \rightarrow ^{10}\text{B}$	3100 ± 31
$^{14}\text{O} \rightarrow ^{14}\text{N}$	3092 ± 4
$^{18}\text{Ne} \rightarrow ^{18}\text{F}$	3084 ± 76
$^{22}\text{Mg} \rightarrow ^{22}\text{Na}$	3014 ± 78
$^{26}\text{Al} \rightarrow ^{26}\text{Mg}$	3081 ± 4
$^{26}\text{Si} \rightarrow ^{26}\text{Al}$	3052 ± 51
$^{30}\text{S} \rightarrow ^{30}\text{P}$	3120 ± 82
$^{34}\text{Cl} \rightarrow ^{34}\text{S}$	3087 ± 9
$^{34}\text{Ar} \rightarrow ^{34}\text{Cl}$	3101 ± 20
$^{38}\text{K} \rightarrow ^{38}\text{Ar}$	3102 ± 8
$^{38}\text{Ca} \rightarrow ^{38}\text{K}$	3145 ± 138
$^{42}\text{Sc} \rightarrow ^{42}\text{Ca}$	3091 ± 7
$^{42}\text{Ti} \rightarrow ^{42}\text{Sc}$	3275 ± 1039
$^{46}\text{V} \rightarrow ^{46}\text{Ti}$	3082 ± 13
$^{46}\text{Cr} \rightarrow ^{46}\text{V}$	2834 ± 657
$^{50}\text{Mn} \rightarrow ^{50}\text{Cr}$	3086 ± 8
$^{54}\text{Co} \rightarrow ^{54}\text{Fe}$	3091 ± 5
$^{62}\text{Ga} \rightarrow ^{62}\text{Zn}$	2549 ± 1280

try to choose the exponents i , j , and k so that $g/m^i \hbar^j c^k$ is dimensionless. A solution immediately follows with $i = -2$, $j = 3$, $k = -1$. Thus the desired ratio, indicated by G , is

$$G = \frac{g}{m^{-2} \hbar^3 c^{-1}} = g \frac{m^2 c}{\hbar^3} \quad (9.31)$$

There is no clear indication of what value to use for the mass in Equation 9.31. If we are concerned with the nucleon-nucleon interaction, it is appropriate to use the nucleon mass, in which case the resulting dimensionless strength constant is $G = 1.0 \times 10^{-5}$. The comparable constant describing the pion-nucleon interaction, denoted by g_π^2 in Chapter 4, is of order unity. We can therefore rank the four basic nucleon-nucleon interactions in order of strength:

pion-nucleon ("strong")	1
electromagnetic	10^{-2}
β decay ("weak")	10^{-5}
gravitational	10^{-39}

(The last entry follows from a similar conversion of the universal gravitational constant into dimensionless form also using the nucleon mass.) The β -decay interaction is one of a general class of phenomena known collectively as *weak interactions*, all of which are characterized by the strength parameter g . The Fermi theory is remarkably successful in describing these phenomena, to the extent that they are frequently discussed as examples of the *universal Fermi*

interaction. Nevertheless, the Fermi theory fails in several respects to account for some details of the weak interaction (details which are unimportant for the present discussion of β decay). A theory that describes the weak interaction in terms of exchanged particles (just as the strong nuclear force was described in Chapter 4) is more successful in explaining these properties. The recently discovered exchanged particles (with the unfortunate name *intermediate vector bosons*) are discussed in more detail in Chapter 18.

The Mass of the Neutrino

The Fermi theory is based on the *assumption* that the rest mass of the neutrino is zero. Superficially, it might seem that the neutrino rest mass would be a reasonably easy quantity to measure in order to verify this assumption. Looking back at Equations 9.1 and 9.2, or their equivalents for nuclei with $A > 1$, we immediately see a method to test the assumption. We can calculate the decay Q value (including a possible nonzero value of the neutrino mass) from Equation 9.6 or 9.9, and we can measure the Q value, as in Equation 9.8, from the maximum energy of the β particles. Comparison of these two values then permits a value for the neutrino mass to be deduced.

From this procedure we can conclude that the neutrino rest mass is smaller than about $1 \text{ keV}/c^2$, but we cannot extend far below that limit because the measured atomic masses used to compute Q have precisions of the order of keV, and the deduced endpoint energies also have experimental uncertainties of the order of keV. A superior method uses the shape of the β spectrum near the upper limit. If $m_\nu \neq 0$ then Equation 9.22 is no longer strictly valid. However, if $m_\nu c^2 \ll Q$, then over most of the observed β spectrum $E_\nu \gg m_\nu c^2$ and the neutrino can be treated in the extreme relativistic approximation $E_\nu \approx qc$. In this case, Equation 9.22 will be a very good approximation and the neutrino mass will have a negligible effect. Near the endpoint of the β spectrum, however, the neutrino energy approaches zero and at some point we would expect $E_\nu \sim m_\nu c^2$, in which case our previous calculation of the statistical factor for the spectrum shape is incorrect. Still closer to the endpoint, the neutrino kinetic energy becomes still smaller and we may begin to treat it nonrelativistically, so that $q^2 = 2m_\nu T_\nu$ and

$$N(p) \propto p^2 \left[Q - \sqrt{p^2 c^2 + m_e^2 c^4} + m_e c^2 \right]^{1/2} \quad (9.32)$$

which follows from a procedure similar to that used to obtain Equation 9.24, except that for $m_\nu > 0$ we must use $dq/dE_\nu = m_\nu/q$ in the nonrelativistic limit. Also,

$$N(T_e) \propto (T_e^2 + 2T_e m_e c^2)^{1/2} (Q - T_e)^{1/2} (T_e + m_e c^2) \quad (9.33)$$

The quantity in square brackets in Equations 9.32 and 9.24, which is just $(Q - T_e)$, vanishes at the endpoint. Thus at the endpoint $dN/dp \rightarrow 0$ if $m_\nu = 0$, while $dN/dp \rightarrow \infty$ if $m_\nu > 0$. That is, the momentum spectrum approaches the

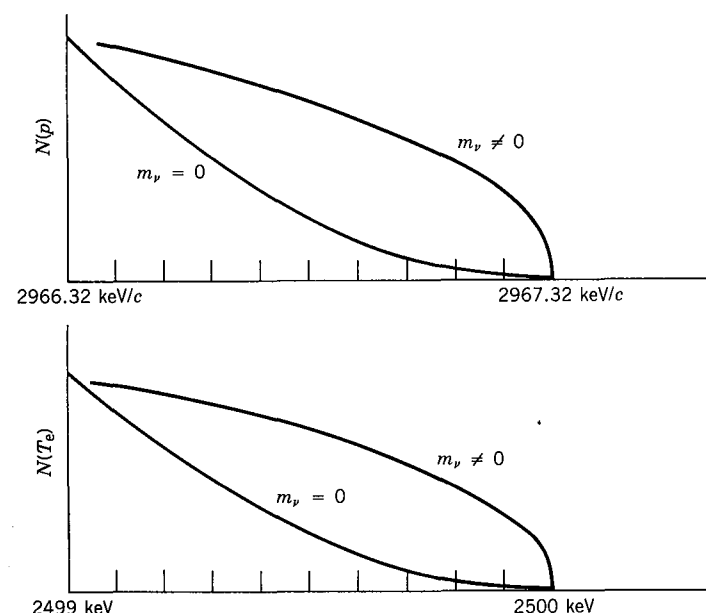


Figure 9.6 Expanded view of the upper 1-keV region of the momentum and energy spectra of Figure 9.2. The normalizations are arbitrary; what is significant is the difference in the shape of the spectra for $m_\nu = 0$ and $m_\nu \neq 0$. For $m_\nu = 0$, the slope goes to zero at the endpoint; for $m_\nu \neq 0$, the slope at the endpoint is infinite.

endpoint with zero slope for $m_\nu = 0$ and with infinite slope for $m_\nu > 0$. The slope of the energy spectrum, dN/dT_e , behaves identically. We can therefore study the limit on the neutrino mass by looking at the slope at the endpoint of the spectrum, as suggested by Figure 9.6. Unfortunately $N(p)$ and $N(T_e)$ also approach zero here, and we must study the slope of a continuously diminishing (and therefore statistically worsening) quantity of data.

The most attractive choice for an experimental measurement of this sort would be a decay with a small Q (so that the relative magnitude of the effect is larger) and one in which the atomic states before and after the decay are well understood, so that the important corrections for the influence of different atomic states can be calculated. (The effects of the atomic states are negligible in most β -decay experiments, but in this case in which we are searching for a very small effect, they become important.) The decay of ^3H (tritium) is an appropriate candidate under both criteria. Its Q value is relatively small (18.6 keV), and the one-electron atomic wave functions are well known. (In fact, the calculation of the state of the resulting ^3He ion is a standard problem in first-year quantum mechanics.) Figure 9.7 illustrates some of the more precise experimental results. Langer and Moffat originally reported an upper limit of $m_\nu c^2 < 200 \text{ eV}$, while two decades later, Bergkvist reduced the limit to 60 eV. One recent result may indicate a nonzero mass with a probable value between 14 and 46 eV, while others suggest an upper limit of about 20 eV. Several experiments are currently being performed to resolve this question and possibly to reduce the upper limit.

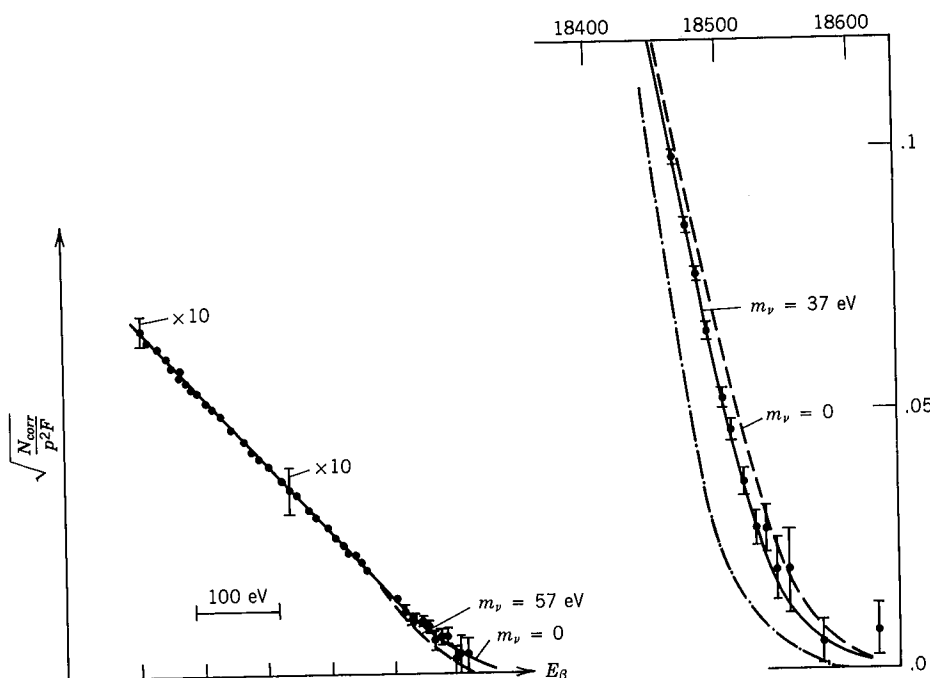


Figure 9.7 Experimental determination of the neutrino mass from the β decay of tritium (^3H). The data at left, from K.-E. Bergkvist, *Nucl. Phys. B* **39**, 317 (1972), are consistent with a mass of zero and indicate an upper limit of around 60 eV. The more recent data of V. A. Lubimov et al., *Phys. Lett. B* **94**, 266 (1980), seem to indicate a nonzero value of about 30 eV; however, these data are subject to corrections for instrumental resolution and atomic-state effects and may be consistent with a vanishing mass.

Why is so much effort expended to pursue these measurements? The neutrino mass has very important implications for two areas of physics that on the surface may seem to be unrelated. If the neutrinos have mass, then the “electroweak” theoretical formalism, which treats the weak and electromagnetic interactions as different aspects of the same basic force, permits electron-type neutrinos, those emitted in β decay, to convert into other types of neutrinos, called muon and τ neutrinos (see Chapter 18). This conversion may perhaps explain why the number of neutrinos we observe coming from the sun is only about one-third of what it is expected to be, based on current theories of solar fusion. At the other end of the scale, there seems to be more matter holding the universe together than we can observe with even the most powerful telescopes. This matter is nonluminous, meaning it is not observed to emit any sort of radiation. The Big Bang cosmology, which seems to explain nearly all of the observed astronomical phenomena, predicts that the present universe should be full of neutrinos from the early universe, with a present concentration of the order of $10^8/\text{m}^3$. If these neutrinos were massless, they could not supply the necessary gravitational attraction to “close” the universe (that is, to halt and reverse the expansion), but with rest masses as low as 5 eV, they would provide sufficient mass-energy density. The study of the neutrino mass thus has direct and immediate bearing not only on nuclear and particle physics, but on solar physics and cosmology as well.

9.4 ANGULAR MOMENTUM AND PARITY SELECTION RULES

Allowed Decays

In the allowed approximation, we replaced the electron and neutrino wave functions with their values at the origin; that is, we regard the electron and neutrino to have been created at $r = 0$. In this case they cannot carry any orbital angular momentum, and the only change in the angular momentum of the nucleus must result from the spins of the electron and neutrino, each of which has the value $s = \frac{1}{2}$. These two spins can be parallel (total $S = 1$) or antiparallel (total $S = 0$). If the spins are antiparallel (which is known as a *Fermi* decay) then in the allowed approximation ($\ell = 0$) there can be no change in the nuclear spin: $\Delta I = |I_i - I_f| = 0$. If the electron and neutrino spins are parallel (which is called a *Gamow-Teller* decay) in the allowed approximation, they carry a total angular momentum of 1 unit and thus I_i and I_f must be coupled through a vector of length 1: $I_i = I_f + 1$. This is possible only if $\Delta I = 0$ or 1 (except for $I_i = 0$ and $I_f = 0$, in which case only the Fermi transition can contribute).

If the electron and neutrino carry no orbital angular momentum, then the parities of the initial and final states must be identical since the parity associated with orbital angular momentum ℓ is $(-1)^\ell$.

We therefore have the following *selection rules* for *allowed β decay*:

$$\Delta I = 0, 1 \quad \Delta\pi \text{ (parity change)} = \text{no}$$

Some examples of allowed β decay are

$^{14}\text{O} \rightarrow ^{14}\text{N}^*$ This $0^+ \rightarrow 0^+$ decay to an excited state of ^{14}N must be pure Fermi type (because $0^+ \rightarrow 0^+$ decays cannot be accomplished through a Gamow-Teller decay, which must carry one unit of angular momentum). Other examples include $^{34}\text{Cl} \rightarrow ^{34}\text{S}$ and $^{10}\text{C} \rightarrow ^{10}\text{B}^*$, both of which are $0^+ \rightarrow 0^+$.

$^6\text{He} \rightarrow ^6\text{Li}$ This decay is $0^+ \rightarrow 1^+$, which must be a pure Gamow-Teller transition. Other allowed pure Gamow-Teller decays include $^{13}\text{B} \rightarrow ^{13}\text{C}$ ($\frac{3}{2}^- \rightarrow \frac{1}{2}^-$), $^{230}\text{Pa} \rightarrow ^{230}\text{Th}^*$ ($2^- \rightarrow 3^-$), and $^{111}\text{Sn} \rightarrow ^{111}\text{In}$ ($\frac{7}{2}^+ \rightarrow \frac{9}{2}^+$).

$n \rightarrow p$ In this case $\Delta I = 0$ ($\frac{1}{2}^+ \rightarrow \frac{1}{2}^+$), and so both the Fermi (F) and Gamow-Teller (GT) selection rules are satisfied. This is an example of a “mixed” F + GT transition, in which the exact proportions of F and GT are determined by the initial and final nuclear wave functions. It is convenient to define the ratio y of the Fermi and Gamow-Teller *amplitudes* (that is, matrix elements):

$$y = \frac{g_F M_F}{g_{GT} M_{GT}} \quad (9.34)$$

where M_F and M_{GT} are the actual Fermi and Gamow-Teller nuclear matrix elements. We allow for the possibility that the Fermi and Gamow-Teller strength constants may differ by defining g_F and g_{GT} as the constants analogous to the single constant g that appears in Equation 9.28. (In the decay rate, we should replace $g^2 |M_{\beta}|^2$ with $g_F^2 |M_F|^2 + g_{GT}^2 |M_{GT}|^2$.) We assume g_F to be identical to the value g deduced from the superallowed ($0^+ \rightarrow 0^+$) Fermi

decays. For neutron decay, the Fermi matrix element can be simply calculated: $|M_F| = 1$. Since the decay rate is proportional to $g_F^2 M_F^2 (1 + y^{-2})$, the neutron decay rate permits a calculation of the ratio y , which yields the value 0.467 ± 0.003 . That is, the decay is 82% Gamow-Teller and 18% Fermi.

In general, the initial and final nuclear wave functions make calculating M_F and M_{GT} a complicated and difficult process, but in one special group of decays the calculation is simplified. That group is the *mirror decays*, which we previously considered in Section 3.1. In decays such as ${}^{41}_{21}\text{Sc}_{20} \rightarrow {}^{41}_{20}\text{Ca}_{21}$, where the 21st proton becomes the 21st neutron, no change of wave function is involved. Except for minor differences due to the Coulomb interaction, the initial and final wave functions are identical, and the calculation of M_F and M_{GT} is easily done. For these nuclei, g_F and M_F have the same values as they do for the decay of the free neutron.

This result may seem somewhat surprising because in a nucleus, a nucleon does not behave at all like a free nucleon, primarily because of the cloud of mesons that surrounds a nucleon as it participates in exchange interactions with its neighbors. The hypothesis that Fermi interactions of nucleons in nuclei are unchanged by the surrounding mesons is called the *conserved vector current* (CVC) hypothesis. (The term “vector” refers to the transformation properties of the operator that causes the Fermi part of the decay; the Gamow-Teller part arises from an “axial vector” type of interaction.) The CVC hypothesis can be understood by analogy with the electromagnetic interaction. The electric charge is not changed by the transformation $p \leftrightarrow n + \pi^+$ which is part of the exchange interaction in which a proton may participate. Electric charge is conserved in this process and the Coulomb interaction is unchanged. (The electrons bound to the nucleus by Coulomb forces are unaware of the transformation.) On the other hand, magnetic interactions are substantially changed by $p \leftrightarrow n + \pi^+$, as we discussed when we considered shell-model magnetic moments in Section 5.1. In β decay, g_F (like electric charge) is unaffected by the surrounding mesons, while g_{GT} (like magnetic moments) may be affected by the meson cloud. In some nuclei, the change amounts to 20–30%. The matrix element M_{GT} also varies with the particular shell model state of the nucleon that makes the transition.

Table 9.3 Ratio of Fermi to Gamow-Teller Matrix Elements

	Decay	$y = g_F M_F / g_{GT} M_{GT}$	%F	%GT
Mirror decays	$n \rightarrow p$	0.467 ± 0.003	18	82
	${}^3\text{H} \rightarrow {}^3\text{He}$	0.479 ± 0.001	19	81
	${}^{13}\text{N} \rightarrow {}^{13}\text{C}$	1.779 ± 0.006	76	24
	${}^{21}\text{Na} \rightarrow {}^{21}\text{Ne}$	1.416 ± 0.012	67	33
	${}^{41}\text{Sc} \rightarrow {}^{41}\text{Ca}$	0.949 ± 0.003	47	53
Nonmirror decays	${}^{24}\text{Na} \rightarrow {}^{24}\text{Mg}$	-0.021 ± 0.007	0.044	99.956
	${}^{41}\text{Ar} \rightarrow {}^{41}\text{K}$	$+0.027 \pm 0.011$	0.073	99.927
	${}^{46}\text{Sc} \rightarrow {}^{46}\text{Ti}$	-0.023 ± 0.005	0.053	99.947
	${}^{52}\text{Mn} \rightarrow {}^{52}\text{Cr}$	-0.144 ± 0.006	2	98
	${}^{65}\text{Ni} \rightarrow {}^{65}\text{Cu}$	-0.002 ± 0.019	< 0.04	> 99.96

Table 9.3 shows a summary of values of the ratio y of the Fermi and Gamow-Teller amplitudes for some mirror nuclei, assuming the CVC hypothesis (g_F is unchanged from its value for neutron decay) and taking $|M_F| = 1$. These values are derived from decay rates.

For decays in which the initial and final wave functions are very different, the Fermi matrix element vanishes, and so measuring the ratio y for these decays is a way to test the purity of the wave functions. Table 9.3 includes some representative values of y for transitions in other than mirror nuclei. These values come from measuring the angular distribution of the β particles relative to a particular direction (similar to studies with α decays discussed in Chapter 8). You can see that the values are in general quite small, showing that the Fermi transitions are inhibited and thus that the wave functions are relatively pure.

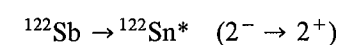
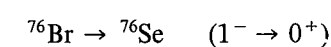
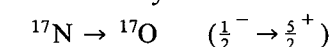
Forbidden Decays

The designation of decays as “forbidden” is really somewhat of a misnomer. These decays are usually less probable than allowed decays (and have generally longer half-lives, as we discuss in the next section), but if the allowed matrix elements happen to vanish, then the forbidden decays are the only ones that can occur.

The most frequent occurrence of a forbidden decay is when the initial and final states have opposite parities, and thus the selection rule for allowed decay is violated. To accomplish the change in parity, the electron and neutrino must be emitted with an odd value of the orbital angular momentum relative to the nucleus. Let us consider, for example, a 1-MeV decay process. If the electron is given all the decay energy, its momentum is 1.4 MeV/c and the maximum angular momentum it can carry relative to the nucleus is $pR = 8.4 \text{ MeV} \cdot \text{fm}/c$ taking $R = 6 \text{ fm}$ as a typical nuclear radius. In units of \hbar , this is equivalent to $pR/\hbar = 0.04$. Thus, while it is less likely to have $\ell = 1$ decays relative to $\ell = 0$, decays with $\ell = 3, 5, 7, \dots$ are extremely unlikely, and we can for the moment consider only those forbidden decays with $\ell = 1$. These are called *first-forbidden* decays, and like the allowed decays they have Fermi types, with the electron and neutrino spins opposite ($S = 0$), and Gamow-Teller types, with the spins parallel ($S = 1$). The coupling of $S = 0$ with $\ell = 1$ for the Fermi decays gives total angular momentum of one unit carried by the beta decay, so that $\Delta I = 0$ or 1 (but not $0 \rightarrow 0$). Coupling $S = 1$ with $\ell = 1$ for the Gamow-Teller decays gives 0, 1, or 2 units of total angular momentum, so that $\Delta I = 0, 1$, or 2. Thus the *selection rules* for first-forbidden decays are

$$\Delta I = 0, 1, 2 \quad \Delta\pi = \text{yes}$$

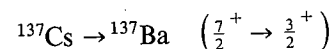
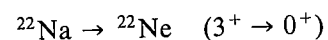
In contrast to the relative simplicity of allowed decays, there are six different matrix elements for first-forbidden decays, and the analysis of decay rates or angular distributions becomes very complicated. We will merely cite some of the many examples of first-forbidden decays:



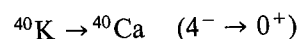
Transitions with $\Delta I \geq 2$, but with no change in parity, are permitted by neither the allowed nor the first-forbidden selection rules. For these transitions we must look to the $\ell = 2$ β emission, and consequently these are known as *second-forbidden* decays. When we couple $S = 0$ or 1 to $\ell = 2$, we can in principle change the nuclear spin by any amount from $\Delta I = 0$ to $\Delta I = 3$ (with certain exceptions, such as $0 \rightarrow 0$ and $\frac{1}{2} \rightarrow \frac{1}{2}$). The $\Delta I = 0$ and 1 cases fall within the selection rules for allowed decays, and we expect that the contribution of the second-forbidden terms to those decays will be negligible (perhaps 10^{-3} to 10^{-4} in angular distributions, and 10^{-6} to 10^{-8} in the spectrum shape). Excepting these cases, the selection rules for the second-forbidden decays are

$$\Delta I = 2, 3 \quad \Delta\pi = \text{no}$$

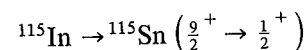
Examples of second-forbidden decays are



Continuing this process, we would find third-forbidden decays ($\ell = 3$), in which the selection rules not also satisfied by first-forbidden processes are $\Delta I = 3$ or 4 and $\Delta\pi = \text{yes}$:



In very unusual circumstances, even fourth-forbidden decays ($\ell = 4$) may occur, with $\Delta I = 4$ or 5 and $\Delta\pi = \text{no}$:



We will learn in the next section that the higher the order of forbiddenness, the more unlikely is the decay. Given the chance, a nucleus prefers to decay by allowed or first-forbidden decays, and higher orders are generally too weak to observe. Only when no other decay mode is possible can we observe these extremely rare third- and fourth-forbidden decays.

9.5 COMPARATIVE HALF-LIVES AND FORBIDDEN DECAYS

Beta-decay half-lives encompass an enormous range, from the order of milliseconds to about 10^{16} years. Part of this variation must be due to the poor match-up of the initial and final nuclear wave functions, but it is hard to imagine that nuclear wave functions are so purely one configuration or another that this effect can account for any but a relatively small part of this variation over 26 orders of magnitude.

The true source of the variation in half-lives is the relative difficulty of creating a β particle and a neutrino in an angular momentum state with $\ell > 0$. As we found in the previous section, a typical (classical) angular momentum for a 1-MeV β particle has a maximum value of the order of $\ell \sim 0.04\hbar$. That is, the probability is very small for the electron and neutrino to be emitted in a state with quantum number $\ell > 0$.

We can make this qualitative estimate more quantitative by considering the wave functions of the electron and neutrino, which are taken to be of the form of plane waves, $e^{i\mathbf{p} \cdot \mathbf{r}/\hbar}$. Expanding the exponential gives $1 + (i\mathbf{p} \cdot \mathbf{r})/\hbar + \frac{1}{2}[(i\mathbf{p} \cdot \mathbf{r})/\hbar]^2 + \dots$. The first term (after sandwiching between the initial and final nuclear wave functions and including the appropriate spin terms) is responsible for *allowed* decays. In the event that the nuclear wave functions cause this term to vanish (they may be of opposite parity, for instance) then we must go to the next term, in which the nuclear part (excepting the spin) is $\int \psi_f^* \mathbf{r} \psi_i dv$. Such terms are responsible for the *first-forbidden* decays. The average value of $\mathbf{p} \cdot \mathbf{r}/\hbar$, integrated over the nuclear volume, is of order 0.01, as we found above. The transition probability is proportional to the square of the integral, and so the probability for first-forbidden decays is only about 10^{-4} that for allowed decays.

The integral also vanishes unless the initial and final states have opposite parities, which can be shown, for example, by writing \mathbf{r} in terms of $Y_1(\theta, \phi)$. This gives again the selection rule $\Delta\pi = \text{yes}$ for first-forbidden decays, as discussed in the previous section.

Each succeeding term in the expansion of the exponential form of the plane wave gives a higher order of forbiddenness, and each gives a transition probability smaller than that of the previous term by a factor of the order of $(\mathbf{p} \cdot \mathbf{r}/\hbar)^2$, or about 10^{-4} .

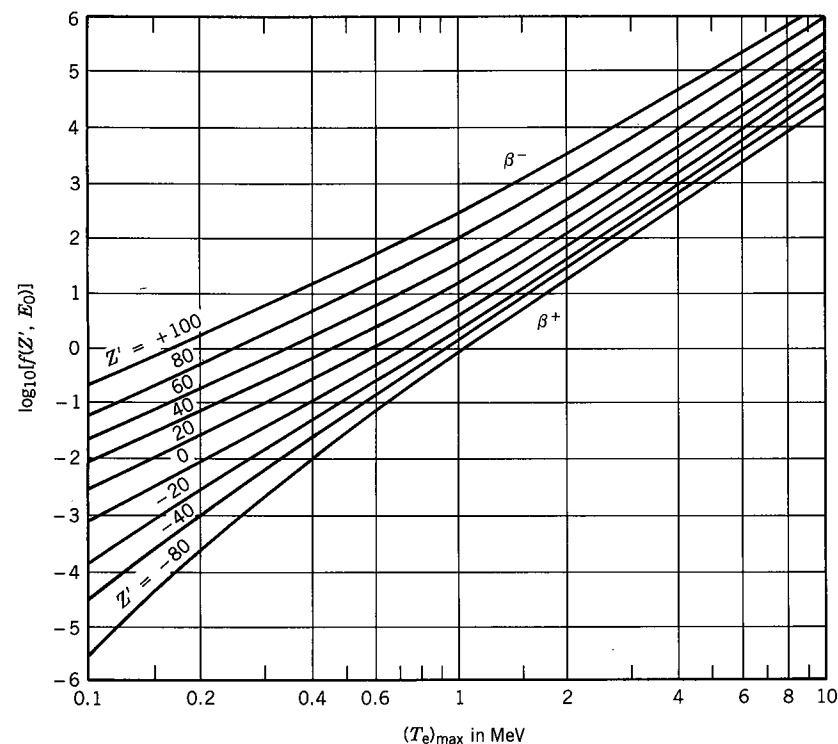


Figure 9.8 The Fermi integral, defined by Equation 9.29. The atomic number Z' refers to the daughter nucleus; the curves for positive Z' are for β^- decay, while negative Z' is for β^+ decay. From R. D. Evans, *The Atomic Nucleus* (New York: McGraw-Hill, 1955).

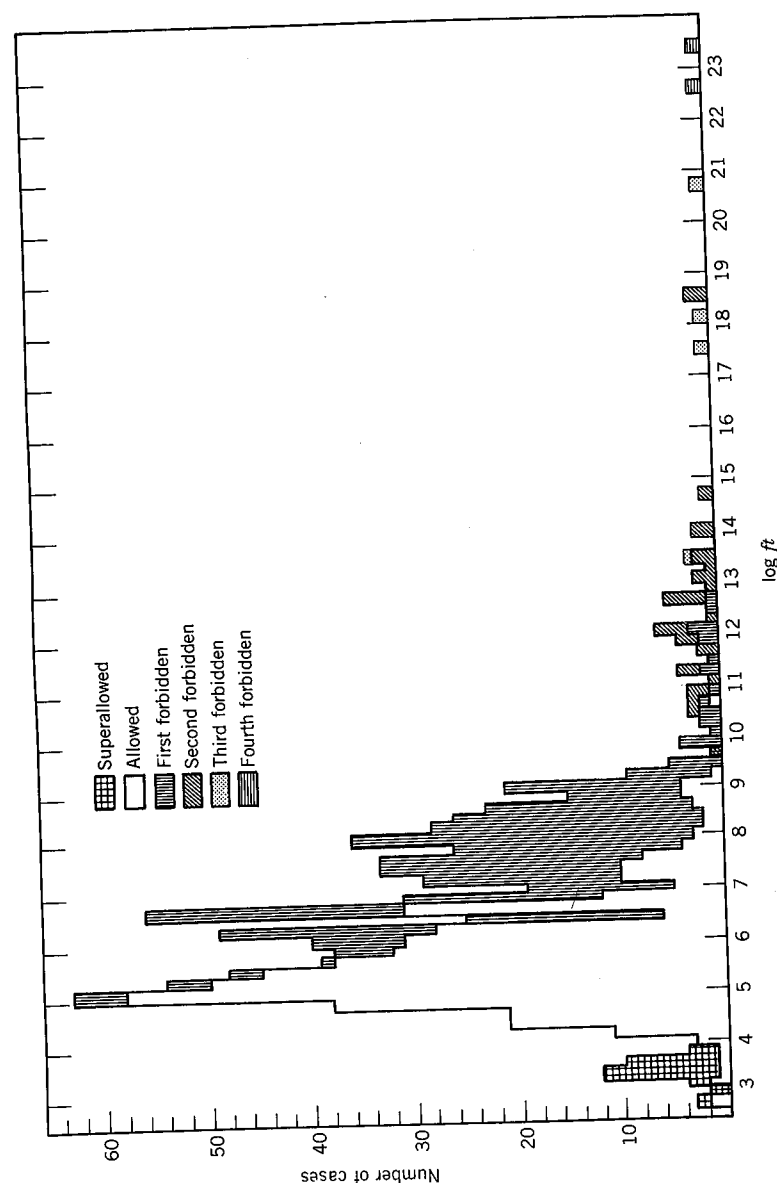


Figure 9.9 Systematics of experimental $\log ft$ values. From W. Meyerhof, *Elements of Nuclear Physics* (New York: McGraw-Hill, 1967).

To compare the half-lives of different β transitions, we must first correct for the variation in the β decay probability that results from differences in the daughter atomic number Z' or in the endpoint energy E_0 . This is done through the *Fermi integral function* $f(Z', E_0)$, which was defined in Section 9.3. If we know the *partial* half-life for a certain decay process, we can find $f(Z', E_0)$ from curves such as those of Figure 9.8. The product $ft_{1/2}$ is the *comparative half-life* or *ft* value, which is usually given as $\log_{10} ft$, where $t_{1/2}$ is always in seconds.

As an example, we consider the β^- decay of ^{203}Hg . The half-life is 46.8 days, so $\log_{10} t_{1/2} = 6.6$. The Q value for the decay to ^{203}Tl is 0.491 MeV. However, essentially 100% of the decay goes to the 279-keV excited state of ^{203}Tl , and so the β endpoint energy will be $0.491 - 0.279 = 0.212$ MeV. From Figure 9.8 we estimate $\log_{10} f = -0.1$, and thus

$$\log_{10} ft = \log_{10} f + \log_{10} t_{1/2} = -0.1 + 6.6 = 6.5$$

For a second example, we take the β^+ decay of ^{22}Na to the ground state of ^{22}Ne ($Z' = 10$). The half-life is 2.60 years but the branching ratio to the ground state is only 0.06%. Thus the partial half-life is $2.60 \text{ years} / 6 \times 10^{-4}$, so that $\log_{10} t_{1/2} = 11.1$. The Q value for β^+ decay is 1.8 MeV, so from Figure 9.8 we estimate $\log_{10} f = 1.6$, and $\log_{10} ft = 11.1 + 1.6 = 12.7$.

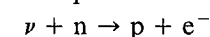
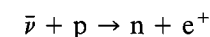
In compilations of nuclear decay information, the $\log ft$ values are given directly. We can determine the type of decay (allowed, n th-forbidden) based on the angular momentum and parity selection rules, and we can then try to relate the experimental $\log ft$ values with the order of forbiddenness. Figure 9.9 summarizes the experimental values of $\log ft$ for different types of decays, and you can see that there is indeed an effect of the order we estimated—each additional degree of forbiddenness increases the $\log ft$ value by about 3.5, representing a reduction in the transition probability by 3×10^{-4} . (There is also a great deal of scatter within each type of decay, a large part of which is probably due to the effects of the particular initial and final nuclear wave functions.)

Most allowed decays have $\log ft$ values in the range 3.5 to 7.5, and first-forbidden decays generally fall in the range 6.0 to 9.0. There are relatively fewer known second-forbidden decays, which have $\log ft$ values from about 10 to 13, and the third-forbidden decays (four cases) range from about 14 to 20. There are two known fourth-forbidden decays, with $\log ft$ about 23.

The value of summaries of this kind of information is in their *predictive ability*; for example, if we are studying a previously unknown decay scheme for which we measure $\log ft = 5.0$, the decay is most probably of the allowed type, which permits us to assign the initial and final states the same parity and to conclude that their spins differ by at most one unit. We shall see the value of such deductions when we discuss β spectroscopy in Section 9.10.

9.6 NEUTRINO PHYSICS

A process closely related to β decay is capture of a neutrino (or an antineutrino) by a nucleon:



which sometimes is called *inverse β decay*.

Let's first discuss why only these processes occur and not others such as capture of a neutrino by a proton or of an antineutrino by a neutron. Electrons and neutrinos belong to a class of particles called *leptons*; the antiparticles e^+ and $\bar{\nu}$ are *antileptons*. Based on observations of many processes and failure to observe certain others, the *law of lepton conservation* is deduced: the total number of leptons minus antileptons on each side of a decay or reaction process must be the same. Many sensitive searches have been made to find violations of this law, but none have yet been found. The reaction $\nu + p \rightarrow n + e^+$, which conserves electric charge and nucleon number, does not conserve lepton number and is therefore, according to our present understanding of fundamental processes, absolutely forbidden.

The failure to observe such reactions is in fact one of our best indicators that ν and $\bar{\nu}$ are really different particles. The electron and positron differ in the sign of their electric charge (and in properties that depend on electric charge, such as magnetic moment). But ν and $\bar{\nu}$ are uncharged (and as uncharged point particles, have vanishing magnetic moments). They are thus immune from the electromagnetic interaction, which is often used to distinguish particles from antiparticles.

As we discussed in Section 9.1, the existence of the neutrino was inferred from the failure of β decay to conform to the well-established conservation laws of energy and momentum conservation. Direct observation of the neutrinos did not occur until 25 years following Pauli's original proposal. To understand the difficulty of catching the elusive neutrino, we can try to estimate the probability for the basic neutrino capture reaction. Let us, in analogy with Equation 4.27, define the cross section for the reaction $\bar{\nu} + p \rightarrow n + e^+$ as

$$\sigma = \frac{\text{probability per target atom for the reaction to occur}}{\text{incident flux of } \bar{\nu}} \quad (9.35)$$

The reaction probability can be calculated using Fermi's Golden Rule, as in Equation 9.12. For the matrix element V_{fi} we can take $(1/V)gM_{fi}$, as we did in the calculation based on the allowed approximation leading to Equation 9.20. Neglecting the recoil of the neutron, the density of final states comes only from the electron and is given by Equation 9.15. Finally, we can adapt the form of Equation 4.26 for the incident flux of $\bar{\nu}$, using the plane wave form of Equation 9.18 and recalling that the quantity $\hbar k/m$ came from the velocity of the incident particle, which is c for neutrinos. The resulting cross section is thus

$$\sigma = \frac{\frac{2\pi}{\hbar} \frac{g^2}{V^2} |M_{fi}|^2 \frac{4\pi p^2 dp V}{h^3 dE}}{c/V} \quad (9.36)$$

Using $dp/dE = E/c^2 p$ gives

$$\sigma = \frac{2\pi}{\hbar c} g^2 |M_{fi}|^2 \frac{4\pi p E}{c^2 h^3} \quad (9.37)$$

To make a numerical estimate, let us use the nuclear matrix element we found for the case of neutron β decay in Section 9.4, $g^2 |M_{fi}|^2 = g_F^2 (1 + y^{-2}) \approx 5.6 g_F^2$; for g_F we take the value deduced from the superallowed β decays. We choose an incident antineutrino energy of 2.5 MeV, somewhat above the minimum energy of 1.8 MeV needed to initiate the reaction (because $m_p c^2 < m_n c^2$, we must

supply the additional needed mass energy through the incident antineutrino), and thus the electron energy is 1.21 MeV. Putting in all of the numerical factors, the resulting cross section is $1.2 \times 10^{-19} \text{ b} = 1.2 \times 10^{-43} \text{ cm}^2$. We can appreciate this incredibly small cross section (compare with the low-energy nucleon-nucleon scattering cross section of 20 b!) by evaluating the probability for a neutrino to be captured in passing through a typical solid, which contains of the order of 10^{24} protons per cm^3 . The neutrino has a reaction cross section of about 10^{-43} cm^2 for each proton it encounters, and in passing through 1 cm^3 of material a neutrino will encounter about 10^{24} protons. The net reaction probability is $(10^{-43} \text{ cm}^2)(10^{24} \text{ cm}^{-3}) = 10^{-19} \text{ cm}^{-1}$; that is, the reaction probability is about 10^{-19} for each cm of material through which the neutrino passes. To have a reasonable probability to be captured, the neutrino must pass through about 10^{19} cm of material, or about 10 light-years. No wonder it took 25 years to find one!

The actual experimental detection was done through an ingenious and painstaking series of experiments carried out in the 1950s by Reines and Cowan. As a source of $\bar{\nu}$ they used a nuclear reactor, since the neutron-rich fission products undergo negative β decay and consequently emit $\bar{\nu}$. The average emission rate is about 6 $\bar{\nu}$ per fission, and the net flux of $\bar{\nu}$ was about 10^{13} per cm^2 per second. For their neutrino detector, Reines and Cowan used a liquid scintillator (rich in free protons) into which a Cd compound had been introduced. The capture of $\bar{\nu}$ by a proton gives a neutron and a positron; the positron quickly annihilates ($e^- + e^+ \rightarrow 2\gamma$) in the scintillator and gives a flash of light. The neutron travels through the solution and is gradually slowed, until finally it is captured by a Cd nucleus, which has a large neutron-capture cross section. Following the neutron capture, ^{114}Cd is left in a highly excited state, which quickly emits a 9.1-MeV γ ray. The characteristic signal of a $\bar{\nu}$ is thus a light signal from the positron annihilation radiation (0.511-MeV photons) followed about 10 μs later (the time necessary for the neutron to be slowed and captured) by the 9.1-MeV neutron capture γ ray. Using a tank containing of the order of 10^6 cm^3 of scintillator, Reines and Cowan observed a few events per hour that were candidates for $\bar{\nu}$ captures. To determine conclusively that these were indeed $\bar{\nu}$ captures, many additional experiments were necessary, following which the conclusion was inescapable—the $\bar{\nu}$ is a real particle, and not just a figment of Pauli's and Fermi's fertile imaginations.

To demonstrate that $\bar{\nu}$ capture by *neutrons* is not possible, a related experiment was done by Davis and co-workers. They used a large tank of CCl_4 in an attempt to observe $\bar{\nu} + {}^{37}\text{Cl} \rightarrow e^- + {}^{37}\text{Ar}$, again with reactor antineutrons. By purging the tank periodically and searching for the presence of radioactive ${}^{37}\text{Ar}$ in the removed gas, Davis was able to conclude that the reaction was not observed, indicating that ν and $\bar{\nu}$ are in fact different particles.

We are thus resolved to the fact that ν and $\bar{\nu}$ are different particles, but we have not yet specified just what is the fundamental property that distinguishes ν from $\bar{\nu}$. Experimentally, there is one property: all $\bar{\nu}$ have their spin vectors parallel to their momentum vectors, while all ν have spin opposite to momentum. This property is called the *helicity* and is defined to be

$$h = \frac{\mathbf{s} \cdot \mathbf{p}}{|\mathbf{s} \cdot \mathbf{p}|} \quad (9.38)$$

which has the value of $+1$ for $\bar{\nu}$ and -1 for ν . (It is often said that $\bar{\nu}$ is “right-handed” and ν is “left-handed” because the precession of s about p traces out a pattern analogous to the threads of a right-handed screw for $\bar{\nu}$ and of a left-handed screw for ν .) Electrons from β decay have a similar property, with $h = -v/c$ for e^- and $h = +v/c$ for e^+ , but this is not an intrinsic property of all e^+ and e^- , only those emitted in β decay. Electrons in atoms have no definite helicities, nor do positrons that originate from pair production ($\gamma \rightarrow e^+ + e^-$). All ν and $\bar{\nu}$, however, have definite helicities, right-handed for $\bar{\nu}$ and left-handed for ν .

Davis has used a similar technique to observe ν emitted by the sun as a result of fusion processes. (Fusion of light nuclei tends to produce neutron-deficient products, which undergo β^+ decay and thus emit ν rather than $\bar{\nu}$.) To shield against events produced by cosmic rays (a problem in his earlier experiments), Davis has placed his CCl_4 tank at the bottom of a 1500-m deep mine, and has spent more than 10 years counting these solar neutrinos. These are especially important because they come to us directly from the core of the sun, where the nuclear reactions occur; the light we see, on the other hand, comes from the sun's surface and contains relatively little direct information about processes that are now going on in the core.) The expected rate of conversion of ^{37}Cl to ^{37}Ar by solar neutrinos in Davis' tank is about *one atom per day*; yet despite years of heroic efforts, the observed rate is only about one-third of the expected value, which represents either an error in the assumptions made regarding the rate of neutrino emission by the sun (and thus a shortcoming of our present theory of solar processes) or an error in our present theories of properties of the neutrino.

9.7 DOUBLE- β DECAY

Consider the decay of ^{48}Ca (Figure 9.10). The Q value for β^- decay to ^{48}Sc is 0.281 MeV, but the only ^{48}Sc states accessible to the decay would be the 4^+ , 5^+ , and 6^+ states, which would require either fourth- or sixth-forbidden decays. If we take our previous empirical estimate of $\log ft \sim 23$ for fourth-forbidden decays, then (with $\log f \approx -2$ from Figure 9.8) we estimate $\log t \sim 25$ or $t_{1/2} \sim 10^{25}$ s (10^{18} y). It is thus not surprising that we should regard ^{48}Ca as a “stable” nucleus.

An alternative possible decay is the *double- β ($\beta\beta$) decay* $^{48}\text{Ca} \rightarrow ^{48}\text{Ti} + 2e^- + 2\bar{\nu}$. This is a direct process, which does not require the ^{48}Sc intermediate state. (In fact, as we shall discuss, in most of the possible $\beta\beta$ decays, the intermediate state is of greater energy than the initial state and is energetically impossible to reach.) The advantage of this process over the single β decay (in this case) is the $0^+ \rightarrow 0^+$ nature of the transition, which would place it in the superallowed, rather than the fourth-forbidden, category.

We can make a rough estimate of the probability for such decay by rewriting Equation 9.30 for single- β decay as

$$\lambda_\beta = \left(\frac{m_e c^2}{\hbar} \right) \left\{ fg^2 \frac{m_e^4 c^2 |M_{fi}|^2}{2\pi^3 \hbar^6} \right\} \quad (9.39)$$

The first term has a value of approximately $0.8 \times 10^{21} \text{ s}^{-1}$ and can be considered

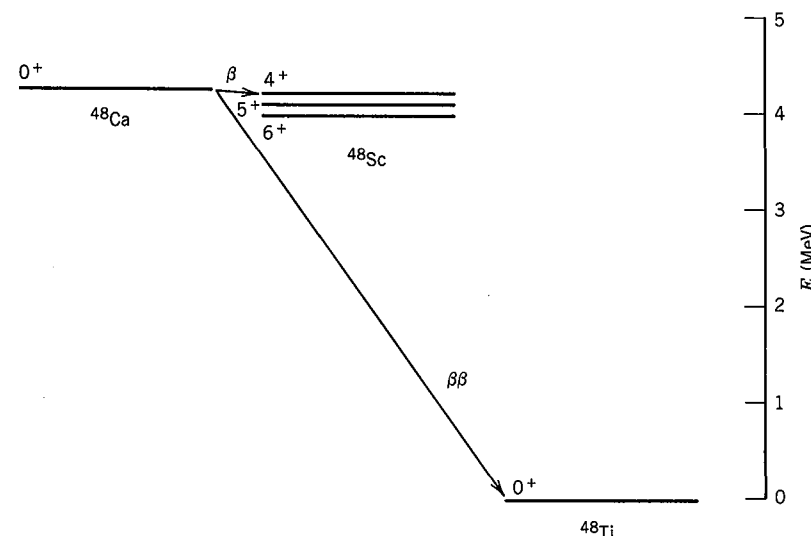


Figure 9.10 The decay of ^{48}Ca . The superallowed $\beta\beta$ decay to ^{48}Ti is an alternative to the fourth-forbidden single- β decay to ^{48}Sc .

the dimensional scaling factor. The remaining term is dimensionless and contains all of the information on the β decay and nuclear transition probabilities. It has a value of $1.5 \times 10^{-25} f$ (using $|M_{fi}| = \sqrt{2}$).

The decay rate for $\beta\beta$ decay then ought to be approximately given by

$$\lambda_{\beta\beta} = \left(\frac{m_e c^2}{\hbar} \right) \left\{ fg^2 \frac{m_e^4 c^2 |M_{fi}|^2}{2\pi^3 \hbar^6} \right\}^2 \quad (9.40)$$

which gives a half-life of the order of 10^{17} years, comparable with the value for single- β decay (although this simple calculation should not be taken too seriously).

Double-beta decay can also occur in cases in which the intermediate state cannot be reached by the single decay mode. Consider the case of ^{128}Te , shown in Figure 9.11. The decay $^{128}\text{Te} \rightarrow ^{128}\text{I}$ has a *negative* Q value of -1.26 MeV, and is therefore not possible. Yet the $\beta\beta$ decay $^{128}\text{Te} \rightarrow ^{128}\text{Xe}$ is energetically possible, with $Q = 0.87$ MeV. In fact, such situations provide the most likely candidates

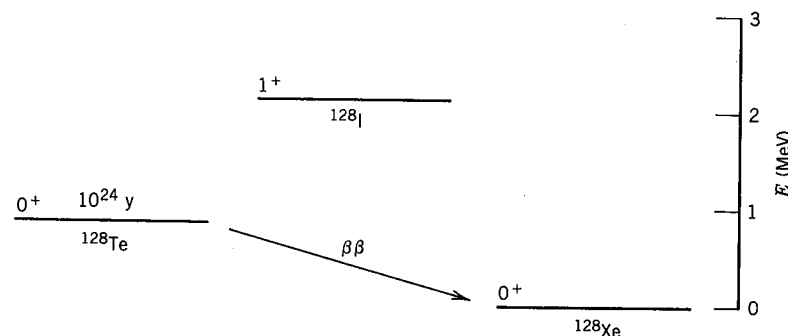


Figure 9.11 Single- β decay of ^{128}Te is energetically forbidden, but $\beta\beta$ decay to ^{128}Xe is possible. See Figure 3.18 to understand the relative masses of these nuclei.

for observing $\beta\beta$ decays because we do *not* want to study the case of two successive decays through an energetically accessible intermediate state.

There are two basic approaches to the observation of $\beta\beta$ decay. The first is the mass spectroscopic method, in which we search for the stable daughter nuclei in minerals of known geological age. If, for example, we were to find an excess abundance of ^{128}Xe (relative to its abundance in atmospheric Xe, for example) in a tellurium-bearing rock, we could deduce an estimate for the $\beta\beta$ -decay half-life of ^{128}Te to ^{128}Xe . Making the reasonable assumption that the $\beta\beta$ -decay half-life is long compared with the age T of the rock, the number of Xe resulting from the $\beta\beta$ decay is

$$N_{\text{Xe}} = N_{\text{Te}}(1 - e^{-\lambda T}) \cong N_{\text{Te}} \frac{0.693T}{t_{1/2}} \quad (9.41)$$

and so

$$t_{1/2} \cong 0.693T \frac{N_{\text{Te}}}{N_{\text{Xe}}} \quad (9.42)$$

The number of Te and Xe nuclei can be determined using mass spectroscopic techniques, and thus the $\beta\beta$ -decay half-life may be found. Some typical values obtained using this method are

$$\begin{aligned} ^{128}\text{Te} \rightarrow ^{128}\text{Xe} & \quad (3.5 \pm 1.0) \times 10^{24} \text{ y} \\ ^{130}\text{Te} \rightarrow ^{130}\text{Xe} & \quad (2.2 \pm 0.6) \times 10^{21} \text{ y} \\ ^{82}\text{Se} \rightarrow ^{82}\text{Kr} & \quad (1.7 \pm 0.3) \times 10^{20} \text{ y} \end{aligned}$$

The direct detection of $\beta\beta$ decay is obviously frustrated by the long half-lives—from one mole of sample, we would expect of the order of one decay per year in the worst case above and one per day in the best case. Experiments with such low count rates always suffer from spurious background counts, such as those from natural radioactivity or cosmic rays, and shielding against these unwanted counts severely taxes the skill of the experimenter. For example, one experiment was done under 4000 m of rock in a tunnel under Mont Blanc on the border between France and Italy!

A recent experiment reported by Moe and Lowenthal used strips of ^{82}Se in a cloud chamber to search for evidence of $\beta\beta$ decays. Figure 9.12 shows examples of a typical event in which two electrons were emitted. Also shown for comparison is another event in which an α particle track originates from the same location as the two electrons; this event probably results from the natural radioactive background, most likely from the decay of ^{214}Bi in the uranium series. A more sensitive search for $\beta\beta$ events by Elliott, Hahn, and Moe, reported in *Phys. Rev. Lett.* **56**, 2582 (1986), showed approximately 30 events possibly associated with $\beta\beta$ decays in more than 3000 h of measuring time. The deduced lower limit on the $\beta\beta$ half-life is 1.0×10^{20} y, in agreement with the geochemical result listed above.

Although the direct method is exceedingly difficult and subject to many possible systematic uncertainties, it is extremely important to pursue these studies because they are sensitive to the critical question of *lepton conservation* (which we

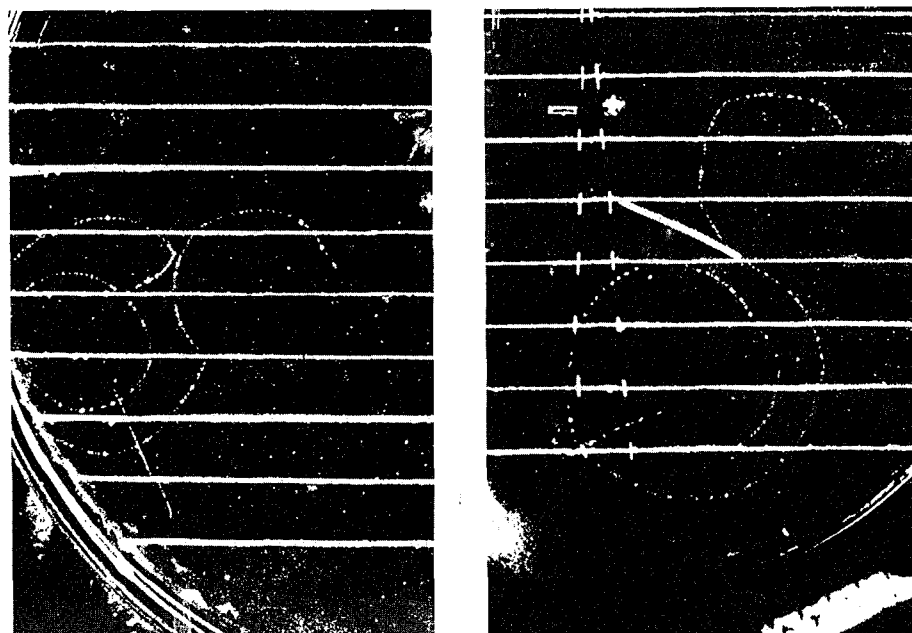
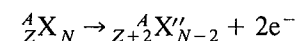


Figure 9.12 Cloud chamber photograph of a suspected $\beta\beta$ -decay event from ^{82}Se . The horizontal lines are strips of ^{82}Se source material. The $\beta\beta$ -decay event is the pair of curved tracks originating from one of the strips in the exact center of the photograph at left. There are also background events due to natural radioactivity; these produce two β -decay electrons in succession (as in the natural radioactive chain of decays, Figure 6.10) and an α particle. Note the two electron tracks and the heavy α track originating from a common point near the center of the photograph on the right. A magnetic field perpendicular to the plane of the photos curves the tracks, so that the electron momentum can be deduced. From M. K. Moe and D. D. Lowenthal, *Phys. Rev. C* **22**, 2186 (1980).

discuss in greater detail in Chapter 18). If ν and $\bar{\nu}$ are not really distinct particles (that is, if they are coupled together or are linear combinations of yet other fundamental particles), then “neutrinoless” $\beta\beta$ decay would be possible:



(In essence, we can think of this process as follows: the first β decay proceeds through the virtual and energetically inaccessible intermediate state ${}^A_{Z+1}\text{X}'_{N-1}$. The emitted $\bar{\nu}$ turns into a ν and is reabsorbed by the virtual intermediate state giving $\nu + {}^A_{Z+1}\text{X}'_{N-1} \rightarrow e^- + {}^A_{Z+2}\text{X}'_{N-2}$. The net process therefore results in the emission of two β 's and no ν 's.)

An experiment designed to search for neutrinoless $\beta\beta$ decay has been done in the case of ^{76}Ge . Here a Ge detector is used both as the source of the decaying nuclei and as the detector of the decays. The total available decay energy is 2.04 MeV, and if the two electrons stop within the detector, it should record a single event with an energy of 2.04 MeV. The difficulty here is to reduce the background (from natural radioactivity, man-made radioactive contaminants, and cosmic rays) to a low enough level so that the 2.04-MeV region can be searched for a

peak. The Mont Blanc experiment mentioned above was of this type and obtained a lower limit on the half-life of 5×10^{21} y. In another underground experiment, reported recently by Avignone et al., *Phys. Rev. C* **34**, 666 (1986), extraordinary measures were taken to surround the detector only with material that would not contribute substantially to the background (stainless steel screws, which showed contamination from ^{60}Co , were replaced with brass, and rubber O-rings were replaced with indium). After 9 months of counting, there was no visible peak at 2.04 MeV, and the half-life was deduced to be greater than 10^{23} y. These experiments are continuing, in the hope that continued improvements in sensitivity will enable both the two-neutrino and the neutrinoless $\beta\beta$ decays to be observed directly.

Although the theoretical interpretations are difficult, it may be that the search for evidence of neutrinoless $\beta\beta$ decay will be an important source of information on the fundamental character of the neutrinos. The emission-reabsorption process described above, for instance, is impossible for massless neutrinos with definite helicities (± 1), and so the observation of the neutrinoless $\beta\beta$ decay would immediately suggest that the "classical" properties of the neutrino are not correct.

9.8 BETA-DELAYED NUCLEON EMISSION

Gamma rays are not the only form of radiation that can be emitted from nuclear excited states that are populated following β decay. Occasionally the states are unstable against the emission of one or more nucleons. The nucleon emission itself occurs rapidly (so that it competes with γ emission), and thus overall the nucleon emission occurs with a half-life characteristic of the β decay.

For decays of nuclei only one or two places from the most stable isobar of each mass number A , the decay energies are small (1–2 MeV), and nucleon emission is forbidden by energetics. Far from the stable nuclei, the decay energies may become large enough to populate highly excited states, which may then decay through nucleon emission. A schematic diagram of this process for proton emission is shown in Figure 9.13. The original β -decaying parent is called the *precursor*; the nucleons themselves come from the *emitter* and eventually lead to states in the *daughter*.

Interest in delayed nucleon emission has increased in recent years in concert with experimental studies of nuclei far from stability. Additional interest comes from the importance of delayed neutrons in the control of nuclear reactors (see Chapter 13). However, the discovery of the phenomenon dates from the early history of nuclear physics—Rutherford in 1916 reported "long-range alpha particles" following the β decay of ^{212}Bi . The main branch in this β decay goes to the ground state of ^{212}Po , which in turn emits α particles with an energy of 8.784 MeV. (Since the α -decaying state is a 0^+ ground state of an even-even nucleus, MeV. (Since the α -decaying state is a 0^+ ground state of an even-even nucleus, the decay proceeds virtually 100% to the ground state of ^{208}Pb .) A small number of α 's, however, were observed with higher energies (9.495 MeV, 0.0035%; 10.422 MeV, 0.0020%; 10.543 MeV, 0.017%). Lower energies would have indicated decays to excited states of ^{208}Pb , but higher energies must indicate decays from excited states of ^{212}Po . Similar behavior was observed in the decay of ^{214}Bi .

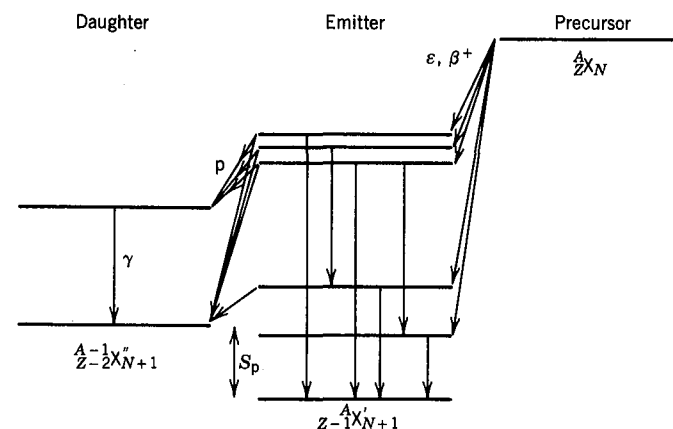


Figure 9.13 Schematic of β -delayed nucleon emission. The β decay of the precursor populates highly excited states in the emitter that are unstable with respect to nucleon emission. Note that the energy of the excited state in the emitter equals the sum of the energy of the emitted nucleon plus the nucleon separation energy between X' and X'' (plus the small correction for the recoil of the emitting nucleus).

The calculation of the energy spectra of the emitted nucleons is a complicated process, requiring knowledge of the spectrum of excited states in the emitter, the probabilities for β decay from the precursor to each state of the emitter, and the probabilities of nucleon decay for each state of the emitter to the accessible states of the daughter. The difficulty is compounded in heavy nuclei by the large density of excited states—the average spacing between excited states at high energy may be of order eV, far smaller than our ability to resolve individual proton or neutron groups; thus all we observe in such cases is a broad distribution, similar in structure to the continuous distribution in β decay but originating from a very different effect. Because of these difficulties, we shall not discuss the theory of delayed nucleon emission; rather, we shall give some examples of experimental studies and their significance.

The energetics of β -delayed nucleon emission are relatively simple. Reference to Figure 9.13 shows immediately that the process can occur as long as the β -decay energy is greater than the nucleon separation energy: $Q_\beta > S_N$ (where $N = n$ or p). Whenever this process is energetically permitted, there will always be competing processes; for example, γ decay of the emitting state or β decays to lower levels in the emitter that cannot decay by particle emission.

The information that we derive from β -delayed nucleon emission is mainly of two types: (1) Since the decay is a two-body process (emitted nucleon plus daughter nucleus), the nucleons emerge with a distinct energy, which gives directly the energy difference between the initial and final states. The energy levels in the daughter are usually well known, and so the energy of the emitted nucleon is in effect a measure of the energy of the excited state of the emitter. (2) From the relative probability of nucleon emission from different states in the emitter, we can deduce the relative population of these states in the β decay of the precursor. This provides information on the β -decay matrix elements. Because the highly excited states in the emitter are so close together, they nearly

form a continuum, and it is more appropriate to consider a β -decay strength function $S_\beta(E_x)$, which gives the average β -decay intensity leading to excited states in the vicinity of excitation energy E_x . Usually there are few selection rules inhibiting β decay to states at this high excitation, and so the β -decay strength function is rather featureless and is roughly proportional to the density of states $\rho(E_x)$. However, there is always one particular state that is so similar in character to the precursor that the majority of the β decays populate that state (it has a particularly large Fermi-type matrix element). The state is known as the *isobaric analog state* (or simply, analog state) because its structure is analogous to the original decaying state in the neighboring isobar. The β -decay strength leading to the analog state (and its energy) can often be determined only through the technique of β -delayed nucleon emission.

As an example of a typical experiment, we consider the β -delayed neutron emission from ^{17}N , which decays by negative β emission to ^{17}O . Figure 9.14 shows three readily identifiable neutron groups, with energies 383, 1171, and 1700 keV; we assume that three excited states of ^{17}O are populated in the β decay and that each emits a neutron to form ^{16}O . Let us assume that these decays go directly to the ground state of ^{16}O . (This is certainly not going to be true in general, but ^{16}O has its first excited state at more than 6 MeV; we will see that it is not possible that the ^{17}N β decay could have enough energy to populate such a highly excited state.)

To analyze the energy transfer in the decay, we first need the neutron separation energy of ^{17}O ; using Equation 3.26:

$$\begin{aligned} S_n &= [m(^{16}\text{O}) - m(^{17}\text{O}) + m_n]c^2 \\ &= (15.99491464 \text{ u} - 16.9991306 \text{ u} + 1.008664967 \text{ u})931.502 \text{ MeV/u} \\ &= 4.144 \text{ MeV} \end{aligned}$$

This is the energy that must be supplied to remove a neutron from ^{17}O . Let's regard the initial state of the system as ^{17}O in an excited state with energy E_x . The initial energy is therefore $m(^{17}\text{O})c^2 + E_x$. The final energy is $m(^{16}\text{O})c^2 + E'_x + m_nc^2 + T_n + T_R$, where T_n is the neutron kinetic energy and T_R is the energy of the ^{16}O recoil, which must occur to conserve momentum. We have included a possible excitation energy of ^{16}O in the term E'_x ; later we will show it must be zero in this case. Energy conservation gives

$$m(^{17}\text{O})c^2 + E_x = m(^{16}\text{O})c^2 + E'_x + m_nc^2 + T_n + T_R$$

or

$$E_x = E'_x + T_n + T_R + S_n \quad (9.43)$$

which is a general result. The recoil correction is obtained by application of conservation of momentum, yielding

$$T_R = T_n \left(\frac{m_n}{m_R} \right) \approx T_n \frac{1}{A-1} \quad (9.44)$$

where m_R is the mass of the recoiling nucleus. Since this is a small correction, we can approximate m_n/m_R by $1/(A-1)$. The final result is

$$E_x = E'_x + \frac{A}{A-1} T_n + S_n \quad (9.45)$$

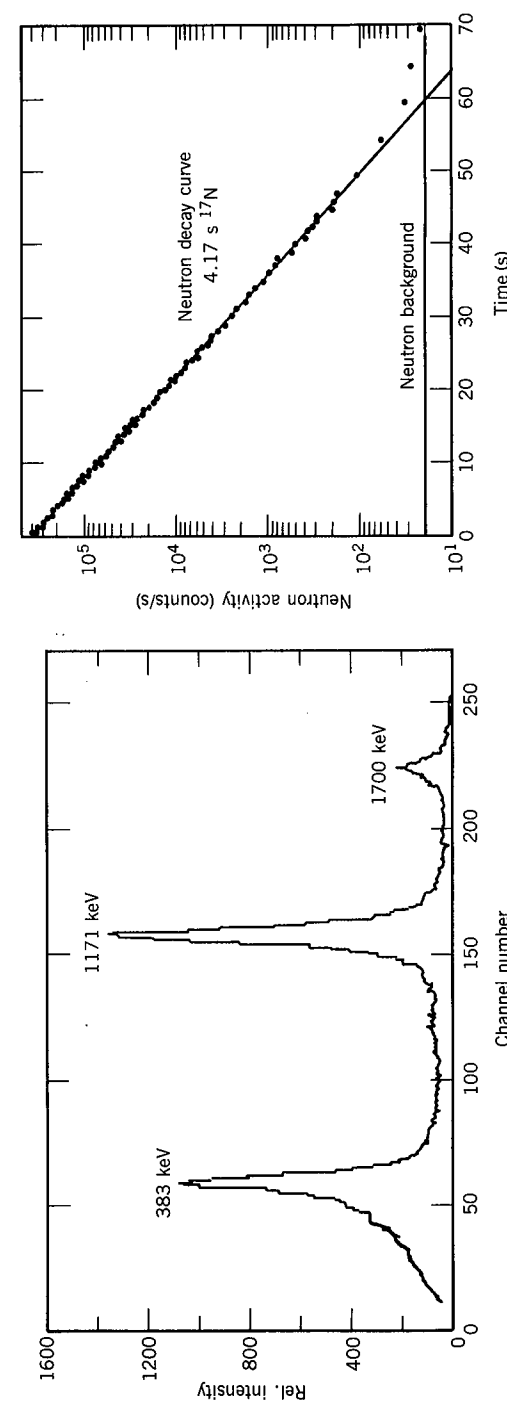


Figure 9.14 Beta-delayed neutrons following the decay of ^{17}N . The neutron energy spectrum is shown at the left; the decay of the neutron activity with time is at the right. From H. Ohm et al., *Nucl. Phys. A* 274, 45 (1976).

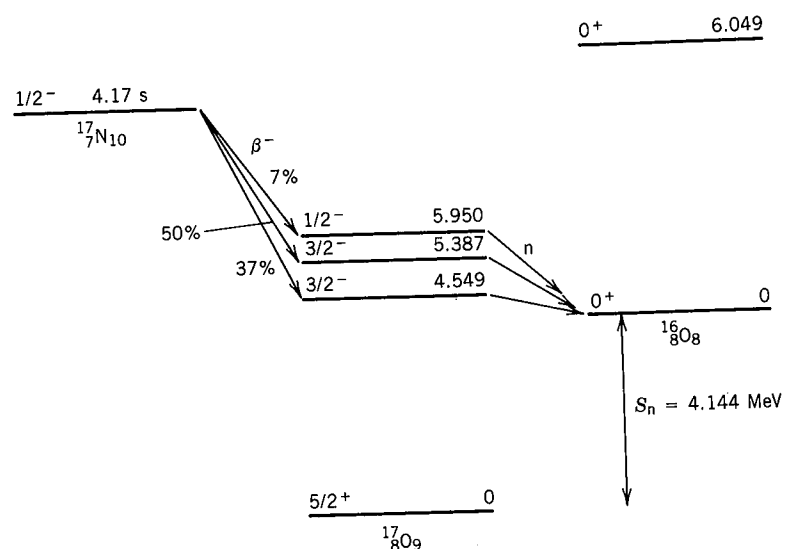


Figure 9.15 The β -delayed neutron decay of ^{17}N .

Assuming $E'_x = 0$ for ^{16}O , the three measured ^{17}N β -delayed neutron energies give excitation energies of 4.551, 5.388, and 5.950 MeV. Nuclear reactions can also be used to measure the energies of the ^{17}O excited states, and three states are found in reaction studies with the energies we have just calculated. If we were to consider the possibility to reach excited states in ^{16}O (that is, $E'_x \geq 6.049$ MeV, the first excited state in ^{16}O), then the lowest possible excitation in ^{17}O would be 10.6 MeV, which is greater than the Q value of the ^{17}N β decay (8.68 MeV). Excited states in ^{16}O are therefore not populated in this decay.

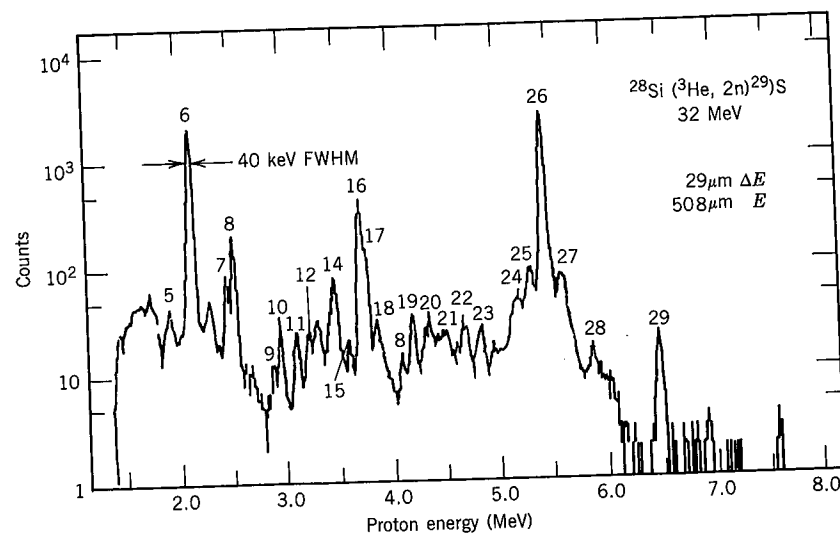


Figure 9.16 Protons emitted following the β decay of ^{29}S . The protons were observed using a $\Delta E \cdot E$ telescope of Si detectors. The numbers refer to specific proton decays of excited state of ^{29}P . Data from D. J. Vieira et al., *Phys. Rev. C* **19**, 177 (1979).

Figure 9.14 also shows the rate of neutron emission as a function of time, which gives the half-life of ^{17}N to be 4.17 s. This half-life is far too long for the decay to be a direct neutron emission process and it must therefore be a β -delayed emission process. The resulting decay is shown in Figure 9.15.

Proton emission will occur most easily from nuclei with an excess of protons, which is certainly the case for ^{29}S ($Z = 16$, $N = 13$). The activity is formed through the reaction $^{28}\text{Si} + ^3\text{He} \rightarrow ^{29}\text{S} + 2n$, which essentially adds two protons and removes a neutron from the stable initial nucleus ($Z = 14$, $N = 14$). The

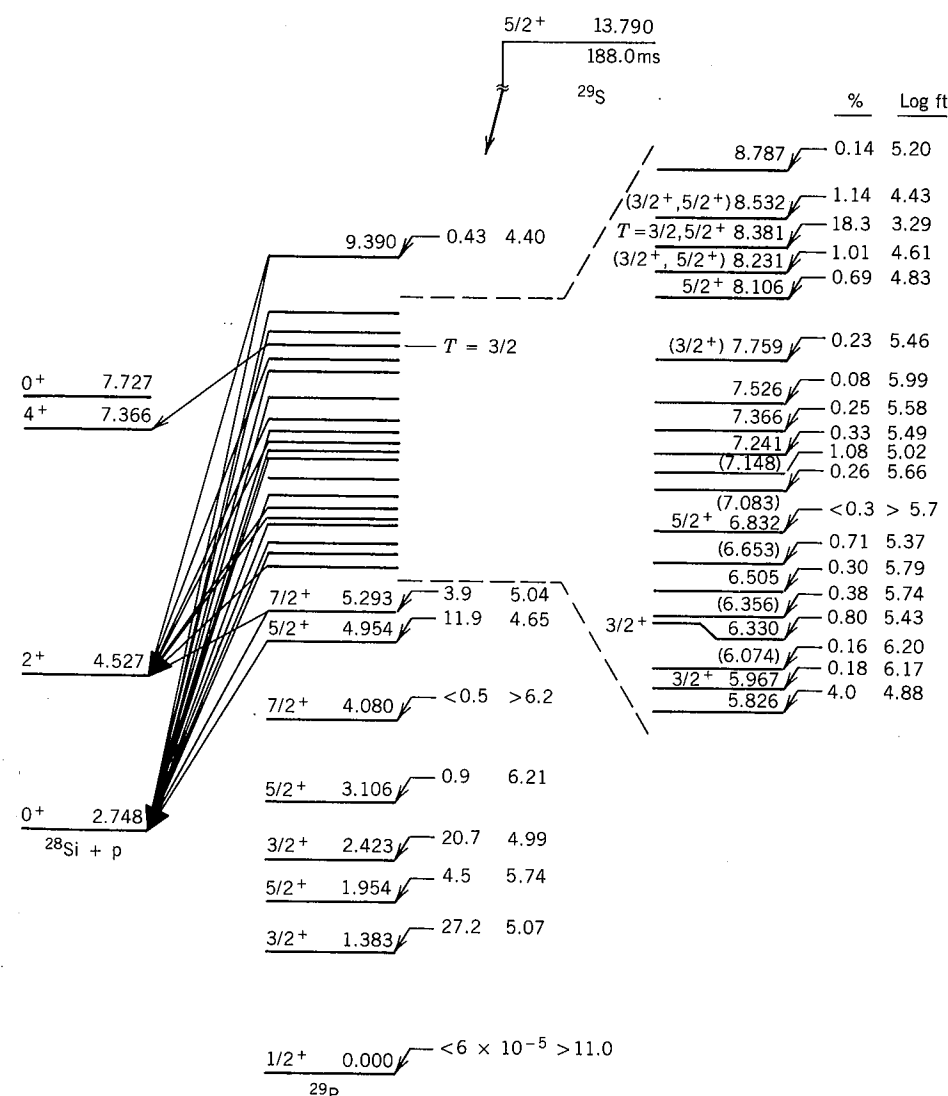


Figure 9.17 Excited states of ^{29}P deduced from the β -delayed proton decay of ^{29}S . The ft values are deduced from the intensity of the observed protons. Note the strong decay branch (small ft value) in the decay to the state at 8.381 MeV, which is the analog state of the ^{29}S ground state.

precursor ^{29}S decays by β^+ emission to states in the emitter ^{29}P , which then emits protons leading to final states in ^{28}Si . Figure 9.16 shows the observed proton spectrum, and Figure 9.17 illustrates the assignment of these proton groups to known initial and final states in ^{29}P and ^{28}Si . Many of the arguments for placing these decays proceed indirectly; for example, the energy difference between the 0^+ ground state and 2^+ first excited state in ^{28}Si is known to be 1.778 MeV, and thus two proton groups differing in energy by 1.778 MeV can be assumed to lead from the same state in the emitter to these two different final states in the daughter (groups 16 and 26, 18 and 27, 22 and 29). The analog state is associated with the strong groups 16 and 26; its $\log ft$ value of 3.29 is characteristic of superallowed decays, as expected for this strongly favored transition.

As we go to heavier nuclei, the density of excited states in the emitter becomes so large that the spacing between levels is smaller than the energy resolution of the detector. When this occurs, it is no longer possible to make the above identification of decays from specific states in the emitter, and only broad, average features of the decay can be discussed (Figure 9.18).

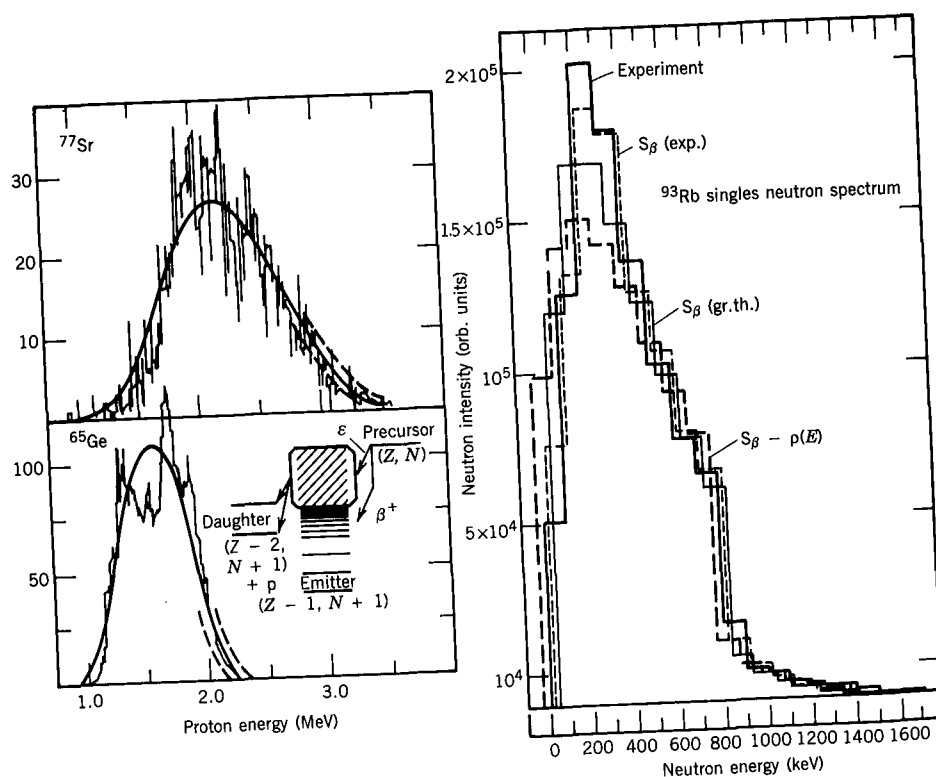


Figure 9.18 Proton (left) and neutron (right) emission following β decay in heavy nuclei. The spacing between excited states in the emitter is so small that we observe only a broad distribution, rather than the individual peaks of Figures 9.14 and 9.16. Attempts to fit the experimental data are based on statistical models, rather than on detailed calculations of individual nuclear states. Proton data from J. C. Hardy et al., *Phys. Lett. B* **63**, 27 (1976); neutron data from K.-L. Kratz et al., *Z. Phys. A* **306**, 239 (1982).

9.9 NONCONSERVATION OF PARITY

The parity operation (as distinguished from the parity quantum number) consists of reflecting all of the coordinates of a system: $\mathbf{r} \rightarrow -\mathbf{r}$. If the parity operation gives us a physical system or set of equations that obeys the same laws as the original system, we conclude that the system is invariant with respect to parity. The original and reflected systems would both represent possible states of nature, and in fact we could not distinguish in any fundamental way the original system from its reflection.

Of course, the macroscopic world *does* show a definite preference for one direction over another—for example, we humans tend to have our hearts on the left side of our bodies. There is no law of nature that demands that this be so, and we could construct a perfectly acceptable human with the heart on the right side. It is the reflection symmetry of the laws of nature themselves with which we are concerned, not the accidental arrangement of the objects governed by the laws.

In fact, there are three different “reflections” with which we frequently work. The first is the spatial reflection $\mathbf{r} \rightarrow -\mathbf{r}$, which is the parity (P) operation. The second “reflection” consists of replacing all particles with their antiparticles; this operation is called *charge conjugation* (C), although there are properties in addition to electric charge that are reversed in this operation. The third operation is *time reversal* (T), in which we replace t by $-t$ and in effect reverse the direction in time of all of the processes in the system. Figure 9.19 shows how three basic processes would appear under the P, C, and T operations. Notice especially that there are some vectors that change sign under P (coordinates, velocity, force, electric field) and some that do not (angular momentum, magnetic field, torque). The former are called true or polar vectors and the latter are pseudo- or axial vectors. Figure 9.20 shows a complete view of a rotating object reflected through the origin. You can see quite clearly that the angular momentum vector does not change direction upon reflection.

In each case shown in Figure 9.19, the reflected image represents a real physical situation that we could achieve in the laboratory, and we believe that gravity and electromagnetism are invariant with respect to P, C, and T.

One way of testing the invariance of the nuclear interaction to P, C, and T would be to perform the series of experiments described in Figure 9.21. In the original experiment, a reaction between particles A and B produces C and D. We could test P by interchanging the particles (for example, have projectile B incident on target A, instead of projectile A incident on target B). We could test C by doing the reaction with antiparticles and T by reacting particles C and D to produce A and B. In each case we could compare the probability of the reversed reaction with that of the original, and if the probabilities proved to be identical, we could conclude that P, C, and T were invariant operations for the nuclear interaction.

In the case of decays $A \rightarrow B + C$, we could perform the same type of tests, as shown in the figure, and could again study the invariance of P, C, and T in decay processes.

We must take care how we test the P operation because, as shown in the figure, the reflected experiment is identical to what we would observe if we turned the page around or stood on our heads to observe the decay or reaction process.

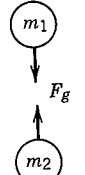
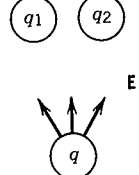
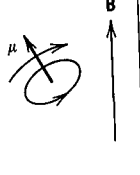
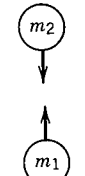
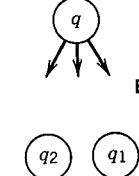
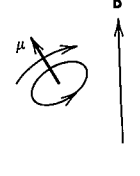
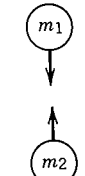
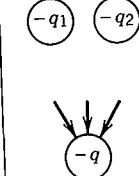
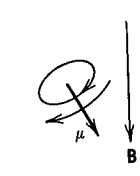
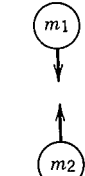
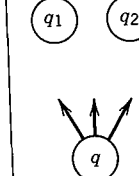
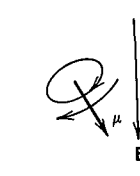
Gravity	Electric field	Magnetic field	
			Original
			P mirror
			C mirror
			T mirror

Figure 9.19 The effect of P, C, and T reversal on gravitational and electromagnetic interactions. In all cases the reversed diagrams represent possible physical situations, and thus these interactions are invariant under P, C, and T.

Since our goal is not to test the invariance of the laws of nature to physicists standing on their heads, we must have some way more clearly to identify the reflected process.

One way is to assume the decaying particle A to have a spin vector that is pointing in a specific direction. The spin does not change direction under P, but it certainly does if we view it upside down. Thus the original experiment shows particle B emitted in the same direction as the spin of A, while the reflected experiment shows B emitted opposite to the spin of A. Quite clearly the experiment differs from its reflection. If, however, we have a large number of A nuclei, all with spins aligned in the same direction, and if they tend to emit B's in equal numbers along the spin and opposite to the spin, then once again the experiment looks like its image. Here then is a way to test P directly—we simply

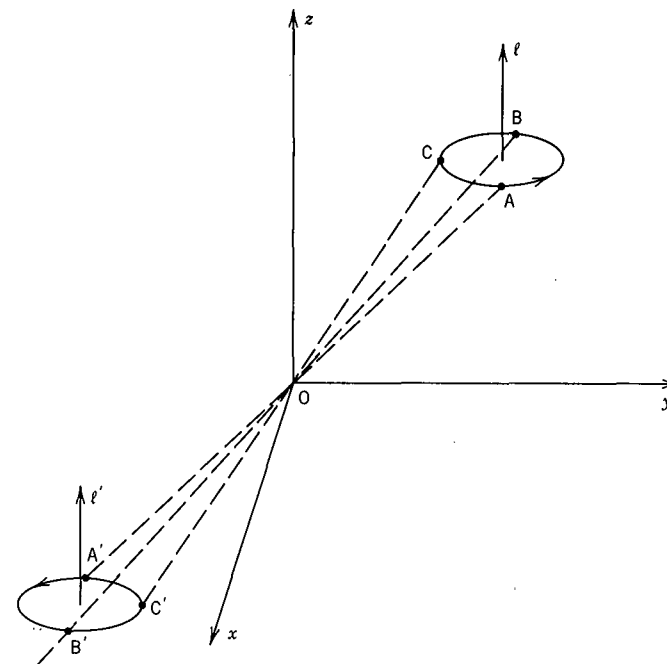


Figure 9.20 The effect of the P operation on a rotating object. If coordinates A, B, and C in the orbit are reflected through the origin ($r \rightarrow -r$), coordinates A', B', and C' result. As the original particle travels from A to B to C, the reflected particle travels from A' to B' to C', and using the right-hand rule to define the direction of the angular momentum indicates that both l and l' point upward. Thus l is a vector that does not change sign under P; such vectors are called *axial vectors*. (Vectors such as r that do change sign under P are called *polar vectors*.)

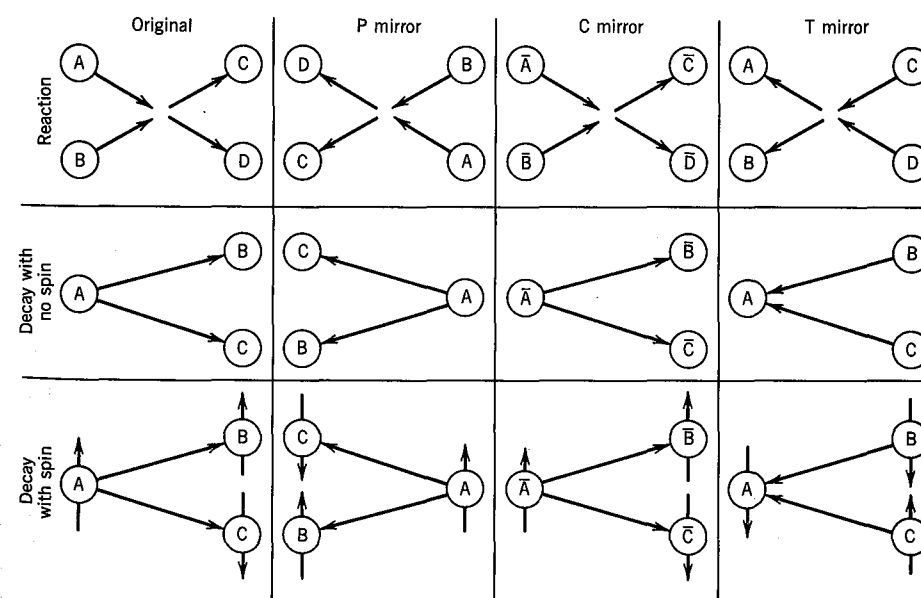


Figure 9.21 Nuclear physics tests of P, C, and T.

align the spins of some decaying nuclei and look to see if the decay products are emitted equally in both directions or preferentially in one direction.

In 1956, T. D. Lee and C. N. Yang pointed out that P had not yet been tested in β decay, even though it had been well tested in other nuclear decay and reaction processes. They were led to this assertion by an unusual situation called the θ - τ puzzle. At that time there were two particles, called θ and τ , which appeared to have identical spins, masses, and lifetimes; this suggested that θ and τ were in fact the same particle. Yet the decays of these particles lead to final states of different parities. Since the decays were governed by a process similar to nuclear β decay, Lee and Yang suggested that θ and τ were the same particle (today called a K meson) which could decay into final states of differing parities if the P operation were not an invariant process for β decay.

Several experimental groups set out to test the suggestion of Lee and Yang, and a successful experiment was soon done by C. S. Wu and her co-workers using the β decay of ^{60}Co . They aligned the ^{60}Co spins by aligning their magnetic dipole moments in a magnetic field at very low temperature ($T \sim 0.01$ K, low enough so that thermal motion would not destroy the alignment). Reversing the magnetic field direction reversed the spins and in effect accomplished the reflection. If β particles would have been observed in equal numbers along and opposite to the magnetic field, then β decay would have been invariant with respect to the P operation. What was observed in fact was that at least 70% of the β particles were emitted opposite to the nuclear spin. Figure 9.22 shows the original data of Wu and colleagues, and you can see quite clearly that the β counting rate reverses as the magnetic field direction is reversed.

Twenty-five years after the original experiment, Wu's research group repeated the ^{60}Co experiment with new apparatus that represented considerably advanced technology for cooling the nuclei, polarizing their spins, and detecting the β particles. Figure 9.23 shows the result of this new experiment, which demonstrates quite clearly the parity-violating effect.

Figure 9.24 shows schematically the ^{60}Co experiment and its reflection in the P mirror. In the P -reflected experiment, the electrons are emitted preferentially along, rather than opposite to, the direction of the magnetic field. Since this represents a state of affairs that is not observed in nature, it must be concluded that, at least as far as β decay is concerned, the P operation is not a valid symmetry. There is yet another surprising result that follows from this experiment. Consider the reflection of the original experiment in the C mirror, also shown in Figure 9.24. The electrons flowing in the wires that produce the magnetic field become positrons, so that the magnetic field reverses. In the C -reflected experiment, the β particles are now emitted preferentially along the magnetic field. Thus matter and antimatter behave differently in beta decay, which is a violation of the C symmetry. (In his book *The Ambidextrous Universe*, Martin Gardner discusses how this experiment can be used to try to decide whether an extraterrestrial civilization, with whom we may someday be in communication, is composed of matter or antimatter.)

If, however, we reflect the experiment in a mirror that simultaneously performs both the P and C operations, as shown in Figure 9.24, the original experiment is restored. Even though the separate C and P operations are not valid symmetries, the CP combination is. (We discuss in Chapter 17 that certain decays of the K

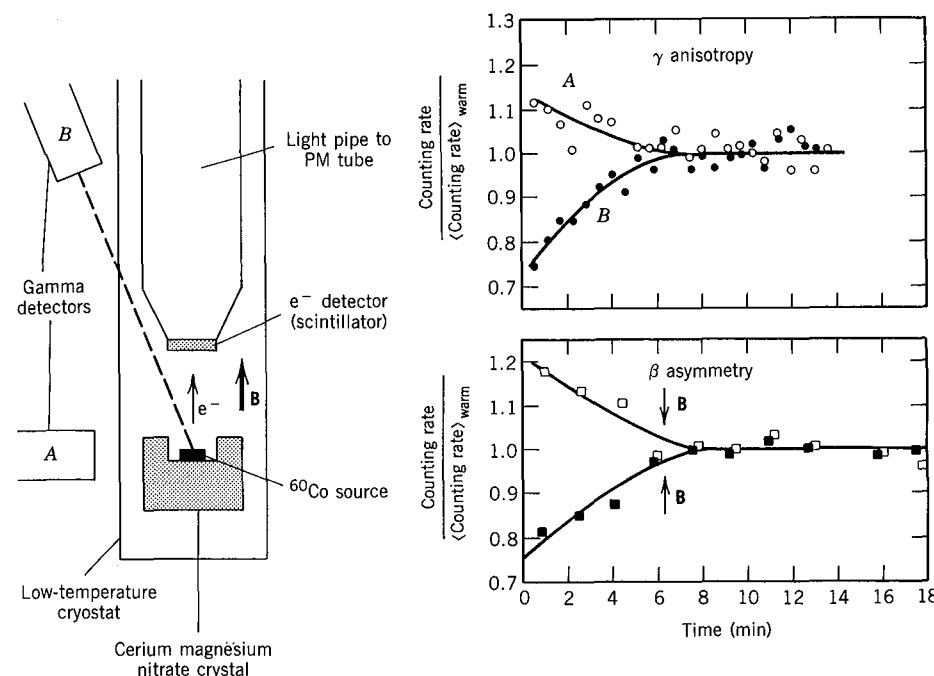


Figure 9.22 Schematic arrangement of experimental test of parity violation in the decay of ^{60}Co . At left is shown the apparatus; the cerium magnesium nitrate crystal is used to cool the radioactive source to about 0.01 K. At bottom right is shown the observed β counting rates; reversing the magnetic field direction is equivalent to subjecting the nuclei to the P operation (see Figures 9.21 and 9.24). If P were not violated, there would be no asymmetry and the field-up and field-down curves would coincide. The vanishing of the asymmetry at about 8 min is due to the gradual warming of the source and the corresponding loss in polarization of the ^{60}Co nuclei, as is demonstrated by the observed γ -ray counting rates. Data from C. S. Wu et al., *Phys. Rev.* **105**, 1413 (1957).

meson, which are analogous to β decays, even violate to a small extent the CP invariance. There is as yet no evidence that the CP symmetry is violated in ordinary nuclear β decay.)

Before we leave this topic, we should discuss the effect of the P nonconservation on nuclear spectroscopy. The interaction between nucleons in a nucleus consists of two parts: the "strong" part, which arises primarily from π meson exchange and which respects the P symmetry, and the "weak" part, which comes from the same interaction responsible for β decay:

$$V_{\text{nuclear}} = V_{\text{strong}} + V_{\text{weak}} \quad (9.46)$$

Typically, the effects of V_{weak} on nuclear spectroscopy are very small compared with those of V_{strong} , but V_{weak} has a property that V_{strong} lacks—it violates the P symmetry. As far as nuclear states are concerned, the effect of V_{weak} is to add to the nuclear wave function a small contribution of the "wrong" parity:

$$\psi = \psi^{(\pi)} + F\psi^{(-\pi)} \quad (9.47)$$

where F is of order 10^{-7} . Under most circumstances, this small addition to the

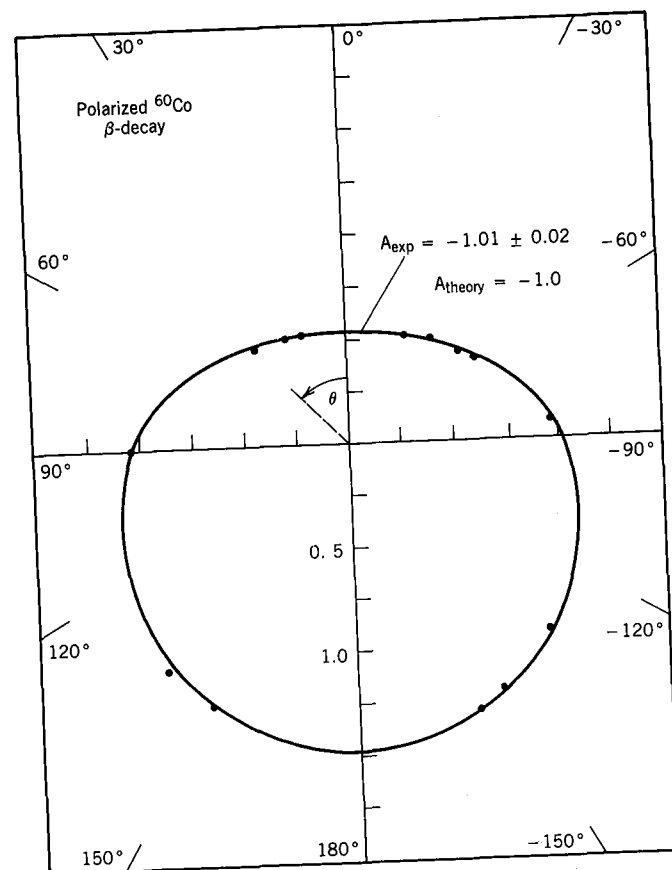


Figure 9.23 Improved results of C. S. Wu and co-workers on the parity violation in the ^{60}Co β decay. The data points (plotted on a polar diagram) give the observed β intensity at an angle θ with respect to the direction of polarization (spin direction) of the decaying ^{60}Co nuclei. The solid curve represents the prediction of the Fermi theory, according to which the intensity should vary as $1 + AP\cos\theta$, where P is a theory, according to which the intensity should vary as $1 + AP\cos\theta$, where P is a parameter that depends primarily on the nuclear polarization. If parity were not violated in β decay, the intensities at 0 and 180° would be equal. From L. M. Chirovsky et al., *Phys. Lett. B* **94**, 127 (1980).

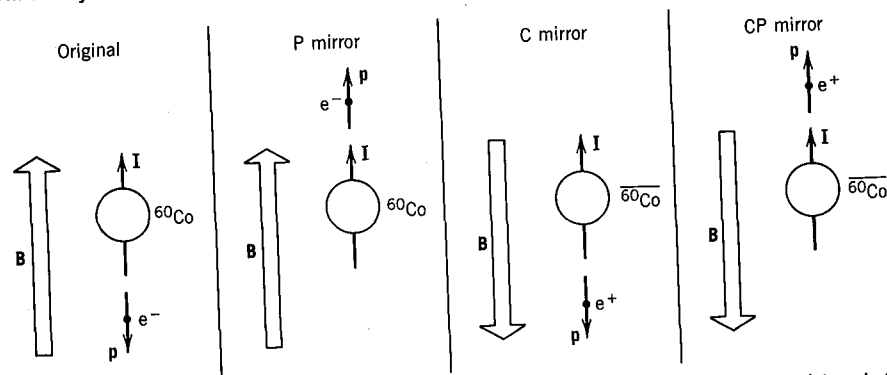


Figure 9.24 The polarized ^{60}Co experiment in the P, C, and combined CP mirrors.

wave function has no observable consequences for nuclear spectroscopy, but there are two cases in particular in which the effects can be observable. In the first, nuclear γ radiation emitted by a polarized nucleus acquires a small difference in intensity between the directions along and opposite to the polarizing magnetic field. This is exactly analogous to the ^{60}Co experiment, but is generally a very small effect (of the order of one part in 10^7) because it arises only from the small part of the wave function and the regular part $\psi^{(\pi)}$ gives no difference in the two intensities. In one very favorable case in the decay of the ^{180}Hf isomeric state, described in K. S. Krane et al., *Phys. Rev. C* **4**, 1906 (1971), the difference is about 2%, but in general it is much smaller and probably beyond our ability to measure. A second type of observation involves the search for a process that would ordinarily be absolutely forbidden if F were zero. For example, consider the α decay of the 2^- level of ^{16}O to the 0^+ ground state of ^{12}C . The selection rules for α decay absolutely forbid $2^- \rightarrow 0^+$ decays (see Section 8.5), but if the 2^- state includes a small piece of 2^+ state, the decay is permitted to occur with a very small intensity proportional to F^2 . Based on a careful study of the α decay of the excited states of ^{16}O , Neubeck et al. discovered a weak branch which they assigned to the parity-violating $2^- \rightarrow 0^+$ transition. The partial half-life for this transition was deduced to be 7×10^{-7} s. By way of comparison, Equation 8.18 gives for the half-life of an ordinary α transition (with $Q = 1.7$ MeV, $B = 3.8$ MeV) the value 2×10^{-21} s. The α decay intensity is thus indeed of order F^2 (10^{-14}), as expected for this P-violating process. A description of this difficult experiment can be found in *Phys. Rev. C* **10**, 320 (1974).

9.10 BETA SPECTROSCOPY

In this section we explore some techniques for deducing the properties of nuclear states (especially excitation energies and spin-parity assignments) through measurements of β decays. This process is complicated by two features of the β -decay process (as compared with α decay, for instance): (1) The β spectrum is continuous. The study of decay processes such as those discussed in Section 8.6 is

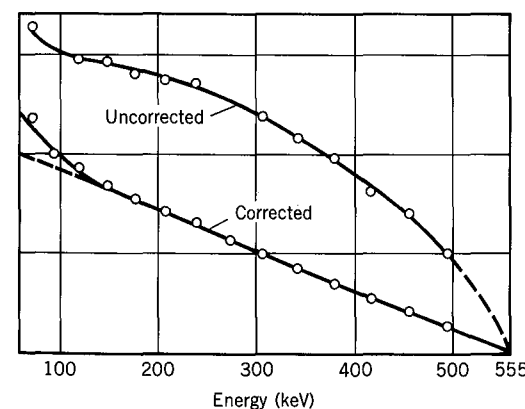
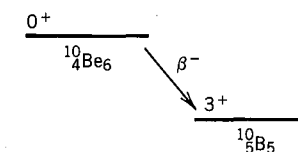


Figure 9.25 Uncorrected Fermi-Kurie plot for ^{10}Be decay and correction for shape factor for second-forbidden transition. Data from L. Feldman and C. S. Wu, *Phys. Rev.* **87**, 1091 (1952).



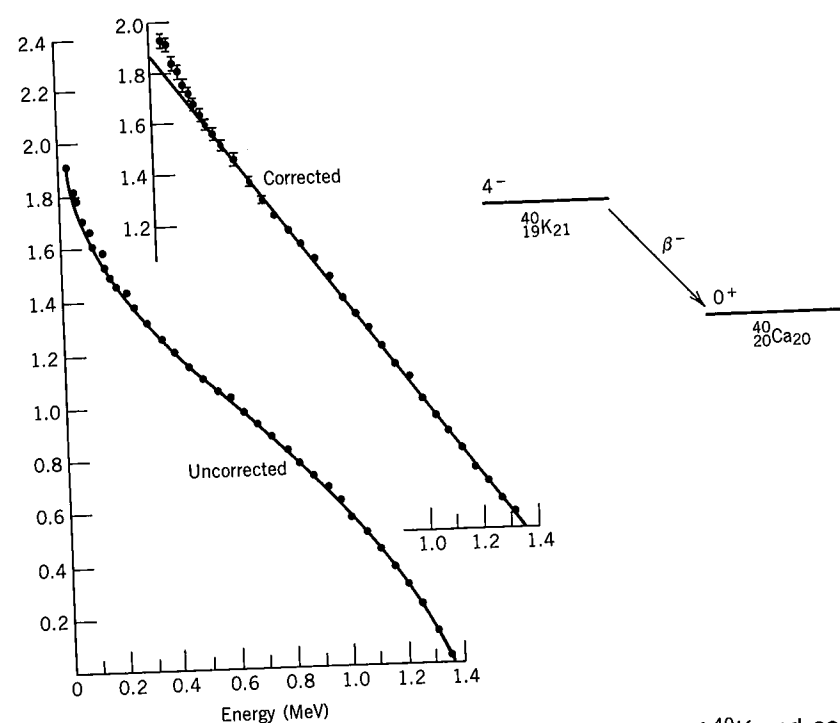


Figure 9.26 Uncorrected Fermi-Kurie plot for the decay of ^{40}K and correction for shape factor of third-forbidden transition. Data from W. H. Kelly et al., *Nucl. Phys.* 11, 492 (1959).

not possible for β decays with many branches, for we cannot reliably “unfold” the various components. (2) The β selection rules are not absolute—the ranges of ft values often overlap and cannot be used to make absolute deductions of decay types, and the measurement of the angular momentum carried by the β particle is not sufficient to fix the relative parities of the initial and final states. There are, however, many cases in which it is possible to derive spectroscopic information from the decays.

Although the shape of the β spectrum and the half-life (actually, the ft value) of the decay are not absolute indicators of the decay type, they do give us strong clues about the type of decay (and therefore the relative spin-parity assignments of the initial and final nuclear states). As discussed in Section 9.3, a linear Fermi-Kurie plot with no shape factor strongly suggests a decay of the allowed type, and we would therefore expect $\Delta I = 0$ or 1 and $\Delta\pi = \text{no}$. A nonlinear Fermi-Kurie plot that is linearized by the shape factor $S = p^2 + q^2$ is, as shown in Figure 9.5, most likely of a first-forbidden type.

Figures 9.25 and 9.26 show additional examples of the use of the shape of the decay to deduce the properties of the initial state. The Fermi-Kurie plot for the decay of ^{10}Be is linearized by a shape factor characteristic of $\Delta I = 3$, $\Delta\pi = \text{no}$ second-forbidden decays. Like all even- Z , even- N nuclei, ^{10}Be has a 0^+ ground state, and so we immediately deduce the assignment of 3^+ for the ^{10}B final state.

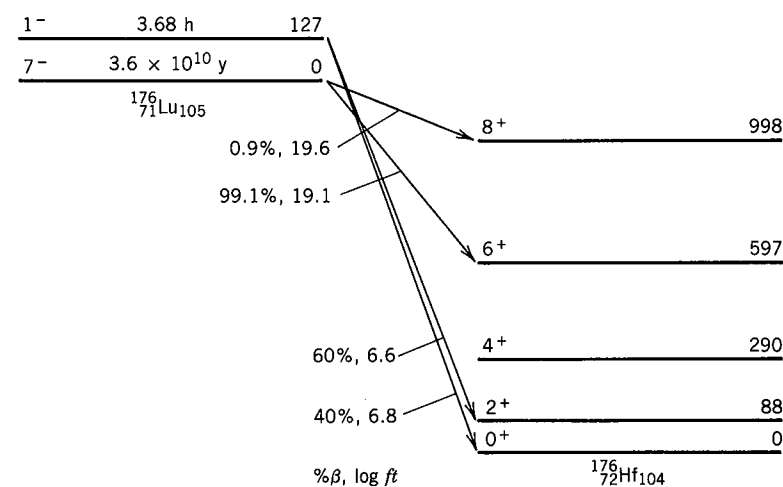


Figure 9.27 The β decay of ^{176}Lu . Level energies are given in keV.

Moreover, the $\log ft$ value of 13.4 is consistent with that expected for second-forbidden decays. The ^{40}K decay proceeds primarily by β^- decay to ^{40}Ca . The Fermi-Kurie plot is linearized by a shape factor characteristic of a $\Delta I = 4$, $\Delta\pi = \text{yes}$ third-forbidden decay. The final state is the ^{40}Ca ground state, which is certainly 0^+ . The initial state is therefore 4^- . The $\log ft$ of 18.1 also suggests a third-forbidden process.

On the other hand, we must be careful not to rely too much on the empirical rules for $\log ft$ values, which are merely based on systematics and not on any theory. In the decay of ^{176}Lu (Figure 9.27) the $\log ft$ is 19.1, while from the known spin-parity assignments we expect a first-forbidden decay (the $\log ft$ values for which usually fall in the range 8–12). It is useful to remind ourselves that a $\log ft$ of 19 means that the β decay is slowed or inhibited by a factor of 10^7 relative to a decay with $\log ft$ of 12. The extreme effect in the ^{176}Lu decay comes about from the unusually poor match of the initial and final nuclear wave functions.

A case in which two different β groups contribute to the decay is illustrated by the decay of ^{72}Zn (Figure 9.28). The weaker group can be reliably seen only through β - γ coincidence measurements. The linear Fermi-Kurie plots and the small $\log ft$ values suggest allowed decays, consistent with the 1^+ assignments to both final states.

A more extreme example comes from the decay of ^{177}Lu (Figure 9.29) in which through careful measurement it is possible to deduce four separate groups. The unfolding procedure begins with the highest group, which is assumed to have a nearly linear Fermi-Kurie plot. Extrapolating the linear high-energy portion backward and subtracting, the remaining spectrum shows an endpoint of 385 keV, and repeating the process reveals two additional components.

We cannot tell directly whether the highest-energy component represents a decay to the ground state of ^{177}Hf , but we can show that it does by computing the Q value for the decay to the ground state. Because ^{177}Lu is radioactive, its mass cannot be measured directly, but we can deduce it through measuring the

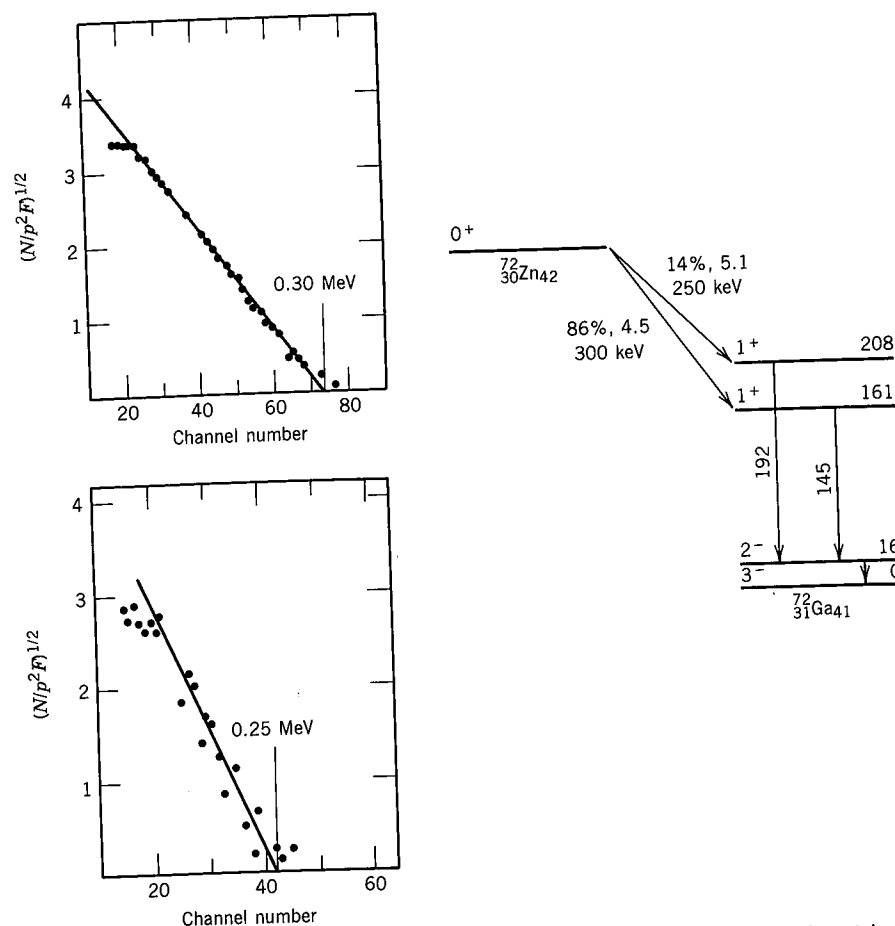


Figure 9.28 β decay of ^{72}Zn . In this case, there are two decays, but the stripping method cannot reliably be used to find the much weaker, lower energy component. At left are shown Fermi-Kurie plots of β 's in coincidence with the 192-keV (bottom) and 145-keV (top) γ rays. The coincidences enable the unambiguous separation of the two decays, the determination of their endpoints, and the demonstration of the linearity of their Fermi-Kurie plots. Data from M. Ishihara, *J. Phys. Soc. Jpn.* **18**, 1111 (1963).

energy released when a low-energy neutron is added to stable ^{176}Lu to form ^{177}Lu . This energy is determined to be 7.0726 ± 0.0006 MeV, and thus

$$\begin{aligned} m(^{177}\text{Lu}) &= m(^{176}\text{Lu}) + m(n) - 7.0726 \text{ MeV}/c^2 \\ &= 176.943766 \pm 0.000006 \text{ u} \end{aligned}$$

where the latter step is made using the known ^{176}Lu mass. We can now find

$$\begin{aligned} Q_\beta &= m(^{177}\text{Lu}) - m(^{177}\text{Hf}) \\ &= 496 \pm 8 \text{ keV} \end{aligned}$$

in excellent agreement with the energy of the highest β group. We therefore conclude that this group populates the ^{177}Hf ground state, with the lower groups

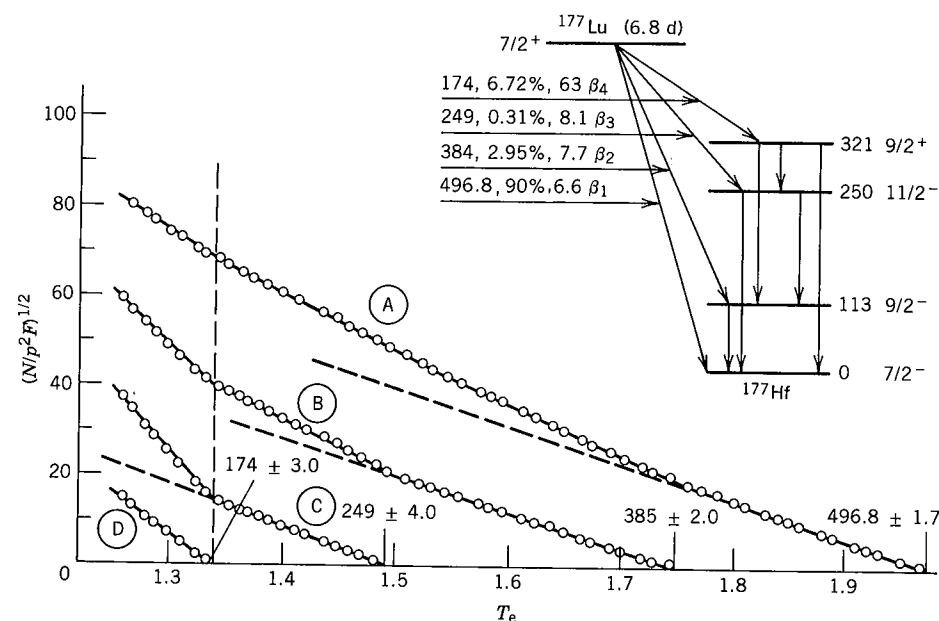


Figure 9.29 Fermi-Kurie plot of the β decay of ^{177}Lu . Curve A represents the complete β spectrum. Extrapolating the high-energy portion (which presumably includes only a single component) gives the dashed line, and the difference between the extrapolated line and curve A gives curve B. The linear portion of curve B gives the endpoint of the next component, and repeating the procedure gives curves C and D. The resulting decay scheme is shown in the inset. Data from M. S. El-Nesr and E. Bashandy, *Nucl. Phys.* **31**, 128 (1962).

populating successively higher states at energies of 112 keV ($= 497 - 385$), 248 keV ($= 497 - 249$), and 323 keV ($= 497 - 174$). The γ spectrum shows results consistent with these deductions, as we discuss in Section 10.8. The 113-keV γ ray, for example, represents the transition from the first excited state to the ground state, and the β spectrum in coincidence with the 113-keV γ ray shows only the 385-keV component.

As a final example of a spectroscopic study, we consider the decay of ^{126}I , which can occur either through negative or positive β emission. The Fermi-Kurie plot (Figure 9.30) is definitely nonlinear at the high end, but when the upper end is corrected by the shape factor for a $\Delta I = 2$, $\Delta\pi = \text{yes}$ first-forbidden decay, it becomes linear and the stripping reveals three groups. Only the two lower groups are in coincidence with γ radiation, suggesting that the highest group populates the ^{126}Xe ground state (0^+) and thus that the decaying state must be 2^- (because the highest group is $\Delta I = 2$, $\Delta\pi = \text{yes}$). The other groups must populate excited states at 385 keV ($= 1250 - 865$) and 865 keV ($= 1250 - 385$). (It is coincidental that the numbers happen to be interchangeable.) The positron spectrum (Figure 9.31) similarly shows two groups which by the same argument populate the ground and first excited (670-keV) state of ^{126}Te . The γ spectrum shows strong transitions of energies 389, 492, 666, 754, 880, and 1420 keV, which can be placed as shown in Figure 9.32, based on the observed β endpoints. The spins of the first excited states are 2^+ , and the second excited states must be 2^+ as well,

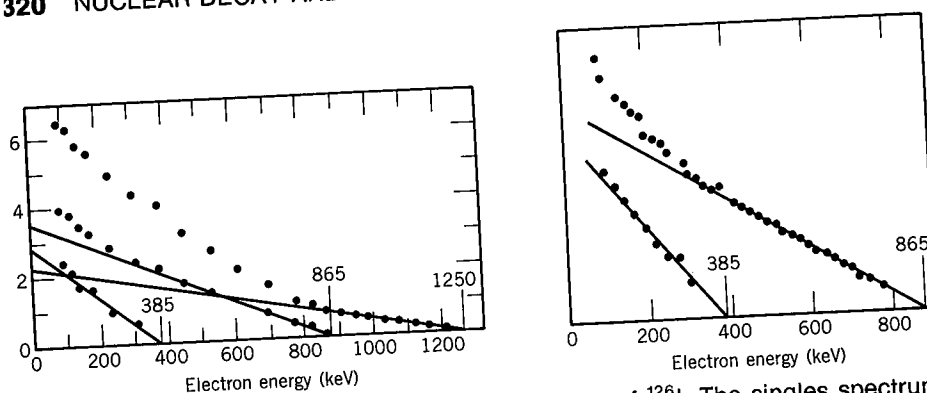


Figure 9.30 Electron spectrum from the β decay of ^{126}I . The singles spectrum (left) shows three components, using a stripping procedure as in Figure 9.29. The coincidence spectrum with gamma radiation (right) does not show the highest energy component; if it is coincident with no γ radiations, it must be a transition to the ground state. Data from L. Koerts et al., *Phys. Rev.* **98**, 1230 (1955).

based on the similarity of the $\log ft$ values and the observed "crossover" transition to the ground state.

The calculation of β matrix elements from nuclear wave functions is a difficult process, and so we usually are content to compare experimental results from different but similar decays. For example, consider the mirror decays of ^{12}B and ^{12}N to ^{12}C (Figure 9.33). The ft values to the different excited states are virtually identical for the β^- and β^+ decays. The transition of the 7th proton into the 6th

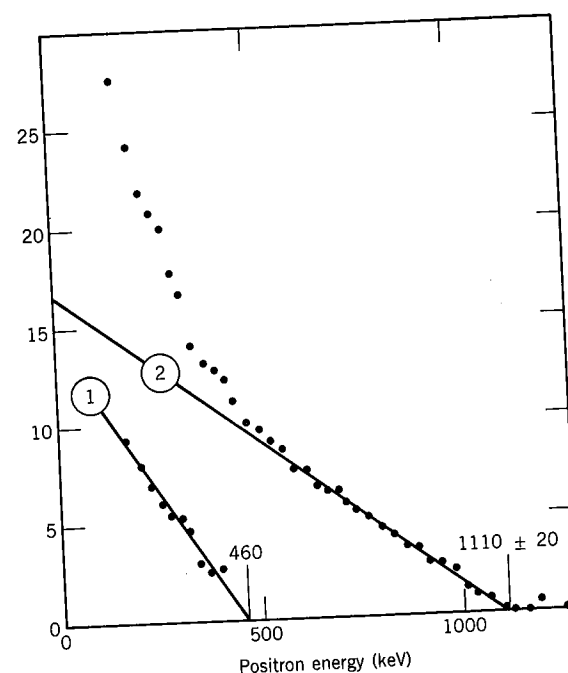


Figure 9.31 Positron spectrum from the β decay of ^{126}I . Stripping reveals two components. Data from L. Koerts et al., *Phys. Rev.* **98**, 1230 (1955).

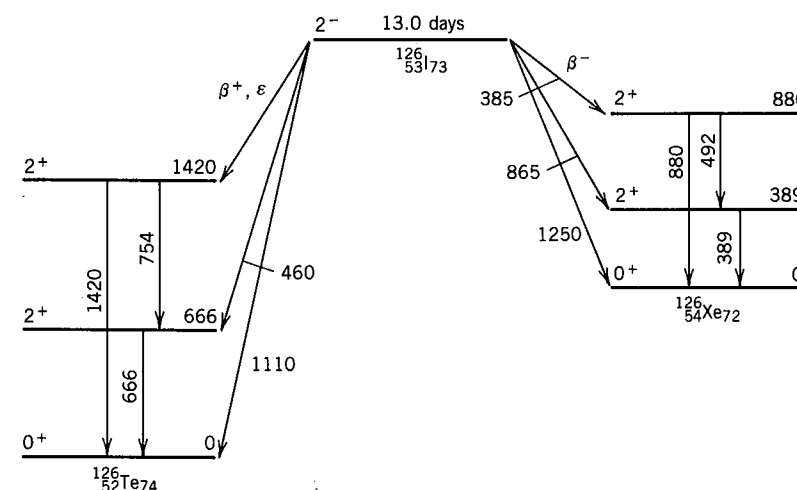


Figure 9.32 Decay scheme of ^{126}I , showing β and γ information. Energies of β 's, γ 's, and levels are given in keV.

neutron would be expected to involve initial and final nuclear wave functions (based on the shell model) identical with those in the transition of the 7th neutron into the 6th proton. The ft values are consistent with this expectation. The transition of the proton into a neutron that leaves the neutron in the same shell-model state as the initial proton results in the population of the 15.11-MeV excited state of ^{12}C . This state therefore has the same nuclear wave functions as the ^{12}B and ^{12}N ground states (except for the difference between protons and neutrons) and is the *analog state* of ^{12}B and ^{12}N . The particularly small ft value in the decay of ^{12}N to this state emphasizes its interpretation as the analog state.

Finally, let's look at the information on nuclear wave functions that can be obtained from β decay. In particular, we examine the transitions between odd neutrons and protons within the $f_{7/2}$ shell. (That is, one $f_{7/2}$ nucleon is transformed into another.) Let us look specifically at cases in odd- A nuclei involving $\Delta I = 0$, allowed decays between states of spin-parity $\frac{1}{2}^-$. The simplest example is

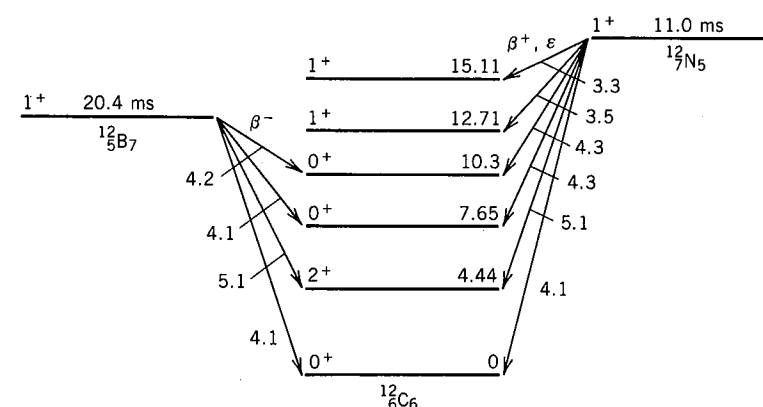


Figure 9.33 Beta decays of ^{12}B and ^{12}N to ^{12}C . Note the similarities in the $\log ft$ values for the β^+ and β^- decays leading to the same final state in ^{12}C .

Table 9.4 β Decays in the $f_{7/2}$ Shell ($\frac{7}{2}^- \rightarrow \frac{7}{2}^-$)

${}^A_ZX_N \rightarrow {}^A_{Z'}X'_{N'}$	$ Z - N' = N - Z' $	$\log ft$
${}^{41}_{21}\text{Sc}_{20} \rightarrow {}^{41}_{20}\text{Ca}_{21}$	0	3.5
${}^{43}_{22}\text{Ti}_{21} \rightarrow {}^{43}_{21}\text{Sc}_{22}$	0	3.5
${}^{45}_{23}\text{V}_{22} \rightarrow {}^{45}_{22}\text{Ti}_{23}$	0	3.6
${}^{53}_{27}\text{Co}_{26} \rightarrow {}^{53}_{26}\text{Fe}_{27}$	0	3.6
${}^{43}_{21}\text{Sc}_{22} \rightarrow {}^{43}_{20}\text{Ca}_{23}$	2	5.0
${}^{45}_{22}\text{Ti}_{23} \rightarrow {}^{45}_{21}\text{Sc}_{24}$	2	4.6
${}^{53}_{26}\text{Fe}_{27} \rightarrow {}^{53}_{25}\text{Mn}_{28}$	2	5.2
${}^{45}_{20}\text{Ca}_{25} \rightarrow {}^{45}_{21}\text{Sc}_{24}$	4	6.0
${}^{47}_{21}\text{Sc}_{26} \rightarrow {}^{47}_{22}\text{Ti}_{25}$	4	5.3
${}^{49}_{23}\text{V}_{26} \rightarrow {}^{49}_{22}\text{Ti}_{27}$	4	6.2
${}^{51}_{24}\text{Cr}_{27} \rightarrow {}^{51}_{23}\text{V}_{28}$	4	5.4
${}^{47}_{20}\text{Ca}_{27} \rightarrow {}^{47}_{21}\text{Sc}_{26}$	6	8.5
${}^{49}_{21}\text{Sc}_{28} \rightarrow {}^{49}_{22}\text{Ti}_{27}$	6	5.7

the decay of ${}^{41}\text{Sc}$ to ${}^{41}\text{Ca}$, in which a single proton outside the doubly magic ${}^{40}\text{Ca}$ core changes into a single neutron. No change of nuclear wave function is involved, and the observed $\log ft$ for this decay is 3.5, placing it in the superallowed category. (This is an example of a *mirror decay*.) In the extreme independent particle shell model, all odd particles are treated equivalently, and we might therefore expect the decay ${}^{47}\text{Ca}$ to ${}^{47}\text{Sc}$ (also $\frac{7}{2}^-$ to $\frac{7}{2}^-$) to show a similar $\log ft$. However, the observed value is 8.5—the decay is slower by a factor of 10^5 ! The transition of the 27th neutron to the 21st proton is thus a more complicated process, and the other six neutrons in the $f_{7/2}$ shell must have a significant influence on the decay. (Some general features of these many-particle states were discussed in Section 5.3.) Table 9.4 summarizes the observed $\frac{7}{2}^-$ to $\frac{7}{2}^-$ β decays of the $f_{7/2}$ shell nuclei ($20 \leq N, Z \leq 28$). You can see that decays in which the odd particle is not required to change its state ($Z - N' = N - Z' = 0$) have $\log ft$ values in the superallowed category (about 3.5); as the value of $Z - N'$ increases, the change of state is correspondingly greater and the $\log ft$ increases, on the average by about one unit (a factor of 10 in the half-life) for each step in $Z - N'$.

REFERENCES FOR ADDITIONAL READING

Other references on “classical” β decay include Chapter 13 of J. M. Blatt and V. F. Weisskopf, *Theoretical Nuclear Physics* (New York: Wiley, 1952); Chapter 17 of R. D. Evans, *The Atomic Nucleus* (New York: McGraw-Hill, 1955); and I. Kaplan, *Nuclear Physics* (Reading, MA: Addison-Wesley, 1955).

More comprehensive reference works, ranging from elementary to advanced material, include H. F. Schopper, *Weak Interactions and Nuclear Beta Decay* (Amsterdam: North-Holland, 1966); C. S. Wu and S. A. Moszkowski, *Beta*

Decay (New York: Wiley-Interscience, 1966); E. J. Konopinski, *The Theory of Beta Decay* (Oxford: Oxford University Press, 1966); M. Morita, *Beta Decay and Muon Capture* (Reading, MA: Benjamin, 1973). An introductory work which includes reprints of some of the classic papers on β decay is C. Strachan, *The Theory of Beta Decay* (Oxford: Pergamon, 1969).

Beta spectroscopy is the subject of C. S. Wu, in *Nuclear Spectroscopy*, part A, edited by F. Ajzenberg-Selove (New York: Academic, 1959), Section I.E.1. A survey of measurements of the shapes of β spectra can be found in H. Daniel, *Rev. Mod. Phys.* **40**, 659 (1968). Many details of β decay are discussed in Chapters 22–24 of *Alpha-, Beta- and Gamma-Ray Spectroscopy*, edited by K. Siegbahn (Amsterdam: North-Holland, 1965).

A general elementary work on neutrino physics is G. M. Lewis, *Neutrinos* (London: Wykeham, 1970). A useful review of the early experimental work can be found in J. S. Allen, *The Neutrino* (Princeton, NJ: Princeton University Press, 1958). A survey of the literature about neutrinos is given in the resource letter of L. M. Lederman, *Am. J. Phys.* **38**, 129 (1970). For a discussion of the solar neutrino experiment, see the article by John Bahcall in the July 1969 issue of *Scientific American*.

Reviews of β -delayed nucleon emission can be found in J. Cerny and J. C. Hardy, *Ann. Rev. Nucl. Sci.* **27**, 333 (1977), and in J. C. Hardy, *Nuclear Spectroscopy and Reactions*, edited by J. Cerny (New York: Academic, 1974), Chapter 8B.

A popular-level treatment of parity is Martin Gardner, *The Ambidextrous Universe* (New York: Scribner, 1979).

Double-beta decay is reviewed in D. Bryman and C. Picciotto, *Rev. Mod. Phys.* **50**, 11 (1978).

PROBLEMS

1. Compute the Q values for the following β^- decays: (a) ${}^{65}\text{Ni} \rightarrow {}^{65}\text{Cu}$; (b) ${}^{11}\text{Be} \rightarrow {}^{11}\text{B}$; (c) ${}^{193}\text{Os} \rightarrow {}^{193}\text{Ir}$.
2. Compute the Q values for the following β^+ and ϵ decays: (a) ${}^{10}\text{C} \rightarrow {}^{10}\text{B}$; (b) ${}^{152}\text{Eu} \rightarrow {}^{152}\text{Sm}$; (c) ${}^{89}\text{Zr} \rightarrow {}^{89}\text{Y}$.
3. ${}^{196}\text{Au}$ can decay by β^- , β^+ , and ϵ . Find the Q values for the three decay modes.
4. The maximum kinetic energy of the positron spectrum emitted in the decay ${}^{11}\text{C} \rightarrow {}^{11}\text{B}$ is 1.983 ± 0.003 MeV. Use this information and the known mass of ${}^{11}\text{B}$ to calculate the mass of ${}^{11}\text{C}$.
5. In the decay of ${}^6\text{He}$ to ${}^6\text{Li}$, the maximum β kinetic energy is 3.510 ± 0.004 MeV. Find the mass of ${}^6\text{He}$, given the mass of ${}^6\text{Li}$.
6. In the decay of ${}^{47}\text{Ca}$ to ${}^{47}\text{Sc}$, what energy is given to the neutrino when the electron has a kinetic energy of 1.100 MeV?
7. The β decay of ${}^{191}\text{Os}$ leads only to an excited state of ${}^{191}\text{Ir}$ at 171 keV. Compute the maximum kinetic energy of the β spectrum.
8. (a) If the β -decay energy is large compared with $m_e c^2$, find a simplified form of Equation 9.25 and show that the average value of T_e (not the value

324 NUCLEAR DECAY AND RADIOACTIVITY

of T_e where $N(T_e)$ has its maximum) is equal to $Q/2$. (b) In the case of β -decay energies that are small compared with $m_e c^2$, show that the average value of T_e is $Q/3$.

9. Supply the missing component(s) in the following processes:

- (a) $\bar{\nu} + {}^3\text{He} \rightarrow$
- (b) ${}^6\text{He} \rightarrow {}^6\text{Li} + e^- +$
- (c) $e^- + {}^8\text{B} \rightarrow$
- (d) $\nu + {}^{12}\text{C} \rightarrow$
- (e) ${}^{40}\text{K} \rightarrow \nu +$
- (f) ${}^{40}\text{K} \rightarrow \bar{\nu} +$

10. What is the kinetic energy given to the proton in the decay of the neutron when (a) the electron has negligibly small kinetic energy; (b) the neutrino has negligibly small energy?

11. One of the processes that is most likely responsible for the production of neutrinos in the sun is the electron-capture decay of ${}^7\text{Be}$. Compute the energy of the emitted neutrino and the kinetic energy of the ${}^7\text{Li}$ nucleus.

12. Defining the Q value as $(m_i - m_f)c^2$, compute the range of neutrino energies in the solar fusion reaction $p + p \rightarrow d + e^+ + \nu$. Assume the initial protons to have negligible kinetic energies.

13. (a) For neutrino capture reactions $\nu + {}^A\text{X} \rightarrow e^- + {}^A\text{X}'$, show that the Q value, defined as in the case of decays as $Q = (m_i - m_f)c^2$, is just $[m({}^A\text{X}) - m({}^A\text{X}')]c^2$ using atomic masses. (b) Neglecting the small kinetic energy given to the final nucleus (to conserve momentum), this Q value is equal to the minimum energy the neutrino must have to cause the reaction. Compute the minimum neutrino energy necessary for capture by ${}^{37}\text{Cl}$, by ${}^{71}\text{Ga}$, and by ${}^{115}\text{In}$. (c) In the Davis experiment (Section 9.6), ${}^{37}\text{Cl}$ is used to detect ν from solar fusion; ${}^{71}\text{Ga}$ and ${}^{115}\text{In}$ have also been proposed as solar neutrino detectors. Comment on the use of these detectors to observe neutrinos from the basic fusion reaction $p + p \rightarrow d + e^+ + \nu$ (see Problem 12) and from the decay of ${}^7\text{Be}$ (see Problem 11).

14. Classify the following decays according to degree of forbiddenness:

- (a) ${}^{89}\text{Sr} (\frac{5}{2}^+) \rightarrow {}^{89}\text{Y} (\frac{1}{2}^-)$
- (b) ${}^{36}\text{Cl} (2^+) \rightarrow {}^{36}\text{Ar} (0^+)$
- (c) ${}^{26}\text{Al} (5^+) \rightarrow {}^{26}\text{Mg}^* (2^+)$
- (d) ${}^{26}\text{Si} (0^+) \rightarrow {}^{26}\text{Al}^* (0^+) \rightarrow {}^{26}\text{Mg} (0^+)$
- (e) ${}^{97}\text{Zr} (\frac{1}{2}^+) \rightarrow {}^{97}\text{Nb}^* (\frac{1}{2}^-)$

15. Show that the slope of the electron energy spectrum for allowed decays is zero near $T_e = Q$ if $m_\nu = 0$ but becomes infinite if $m_\nu \neq 0$.

16. Electron-capture decays can originate with any atomic shell K, L, ... For a wide range of nuclei, the L-capture probability is about 11% of the K-capture probability. Justify this ratio with an estimate based on the probability to locate an orbital electron near the nucleus. For this rough estimate, ignore any effects of electron screening.

17. (a) Consider a $0^+ \rightarrow 0^+ \beta^-$ decay. Using the helicity, Equation 9.38, of the emitted e^- and ν , deduce whether the e^- and ν tend to be emitted parallel

or antiparallel to one another. (b) Repeat for a $1^+ \rightarrow 0^+ \beta^-$ decay. (c) What are the implications of these results for the recoil of the nucleus? (d) Would any of your conclusions differ in the case of β^+ decay?

18. ${}^{20}\text{Na}$ decays to an excited state of ${}^{20}\text{Ne}$ through the emission of positrons of maximum kinetic energy 5.55 MeV. The excited state decays by α emission to the ground state of ${}^{16}\text{O}$. Compute the energy of the emitted α .
19. Following the decay of ${}^{17}\text{Ne}$, a highly excited state in ${}^{17}\text{F}$ emits a 10.597 MeV proton in decaying to the ground state of ${}^{16}\text{O}$. What is the maximum energy of the positrons emitted in the decay to the ${}^{17}\text{F}$ excited state?
20. A certain β -decay process has three components, with maximum energies 0.672, 0.536, and 0.256 MeV. The first component has two coincident γ rays: 0.468 and 0.316 MeV, which are also coincident with each other. The second component has coincident γ 's of 0.604, 0.308, 0.136, 0.468, 0.612, 0.296, and 0.316 MeV. The third β component is in coincidence with all of the above, plus 0.885, 0.589, 0.416, and 0.280 MeV. Use this information to construct a decay scheme and find the mass difference between the nuclear ground states.
21. The decay of ${}^{198}\text{Au}$ to ${}^{198}\text{Pt}$ by electron capture has not been observed, even though the very similar decay of ${}^{196}\text{Au}$ to ${}^{196}\text{Pt}$ by electron capture proceeds strongly. Examine the spectroscopic features of these decays and explain why the ${}^{198}\text{Au}$ electron-capture decay is not observed. (Use the *Table of Isotopes* or a similar spectroscopic reference.)
22. From collections of nuclear spectroscopic data, find and tabulate ft values for $\frac{3}{2}^+ \rightarrow \frac{1}{2}^+$ allowed decays in the region of N or $Z = 14$ to 20 ($d_{3/2}$ and $s_{1/2}$ shells). Also tabulate the allowed $\frac{3}{2}^- \rightarrow \frac{1}{2}^-$ decays for N or $Z = 2$ to 8 ($p_{3/2}$ and $p_{1/2}$ shells). Discuss any systematic differences between the two sets of values.
23. Using systematic collections of nuclear data (such as the *Table of Isotopes* or the *Nuclear Data Sheets*), tabulate the available information on $0^+ \rightarrow 0^+ \beta$ transitions between $f_{7/2}$ nuclei ($20 \leq Z, N \leq 28$). Discuss the coupling of the odd proton and odd neutron, and explain the observed ft values.
24. Tabulate the available information on $g_{9/2} \rightarrow g_{7/2}$ positron decays of odd-mass nuclei; $g_{9/2}$ protons are generally found in the range $40 \leq Z \leq 50$, and $g_{7/2}$ neutrons are usually between $N = 50$ and $N = 66$. Try to account for the ft values. (Note: The GT decay is sometimes called a "spin-flip" process.)
25. There are many β -decaying odd- Z , odd- N nuclei with 2^- spin-parity assignments. These can decay to the 0^+ ground state or the 2^+ first excited state of the neighboring even- Z , even- N nucleus. (a) Use a general nuclear spectroscopy reference (*Table of Isotopes* or the *Nuclear Data Sheets*) to tabulate the ft values for the 2^+ and 0^+ final states from as many of these decay processes as you can find. (b) The $2^- \rightarrow 0^+$ decay is a first-forbidden process, in which the β decay must carry 2 units of total angular momentum, while in the $2^- \rightarrow 2^+$ decay it can carry 0, 1, or 2 units of angular momentum. Use your compilations of ft values to make some general conclusions on the relative probability of the β decay carrying 2 units of

angular momentum. (c) To examine whether there might be an explanation for this effect in terms of the 0^+ and 2^+ nuclear wave functions, make a similar tabulation of decays from 1^- states, that is, of $1^- \rightarrow 0^+$ and $1^- \rightarrow 2^+$ decays. Both these first-forbidden decays carry one unit of total angular momentum. (Why?) Do you observe a systematic difference in ft values between 0^+ and 2^+ final states? What do you conclude about the probable effect of the final nuclear state on the β decays from 2^- initial states?

26. There are several examples of allowed β decays that have larger than average ft values, which can be explained with reference to the nuclear structure. Consider, for example, the following cases: (a) $^{65}\text{Ni} \rightarrow ^{65}\text{Cu}$ and $^{65}\text{Zn} \rightarrow ^{65}\text{Cu}$, in which the ground state-ground state decays are both $\frac{5}{2}^-$ to $\frac{3}{2}^-$ Gamow-Teller decays, but the ft values are 1–2 orders of magnitude larger than for allowed decays to other low-lying states; (b) $^{115}\text{Te} \rightarrow ^{115}\text{Sb}$ and $^{115}\text{Sb} \rightarrow ^{115}\text{Sn}^*$; in the ^{115}Te decay, the $\frac{7}{2}^+ \rightarrow \frac{5}{2}^+$ transition to the ^{115}Sb ground state is not seen, and in the ^{115}Sb decay, a $\frac{7}{2}^+$ low-lying excited state is populated only weakly, with an ft value again 1–2 orders of magnitude larger than values for neighboring excited states. Find the shell model identification of these states and thus explain why the allowed decay mode is inhibited. Use the *Table of Isotopes* to find other examples of inhibited decays with the same shell-model assignments.

10

GAMMA DECAY

Most α and β decays, and in fact most nuclear reactions as well, leave the final nucleus in an excited state. These excited states decay rapidly to the ground state through the emission of one or more γ rays, which are photons of electromagnetic radiation like X rays or visible light. Gamma rays have energies typically in the range of 0.1 to 10 MeV, characteristic of the energy difference between nuclear states, and thus corresponding wavelengths between 10^4 and 100 fm. These wavelengths are far shorter than those of the other types of electromagnetic radiations that we normally encounter; visible light, for example, has wavelengths 10^6 times longer than γ rays.

The detail and richness of our knowledge of nuclear spectroscopy depends on what we know of the excited states, and so studies of γ -ray emission have become the standard technique of nuclear spectroscopy. Other factors that contribute to the popularity and utility of this method include the relative ease of observing γ rays (negligible absorption and scattering in air, for instance, contrary to the behavior of α and β radiations) and the accuracy with which their energies (and thus by deduction the energies of the excited states) can be measured. Furthermore, studying γ emission and its competing process, internal conversion, allows us to deduce the spins and parities of the excited states.

10.1 ENERGISTICS OF γ DECAY

Let's consider the decay of a nucleus of mass M at rest, from an initial excited state E_i to a final state E_f . To conserve linear momentum, the final nucleus will not be at rest but must have a recoil momentum p_R and corresponding recoil kinetic energy T_R , which we assume to be nonrelativistic ($T_R = p_R^2/2M$). Conservation of total energy and momentum give

$$\begin{aligned} E_i &= E_f + E_\gamma + T_R \\ 0 &= p_R + p_\gamma \end{aligned} \quad (10.1)$$

It follows that $p_R = p_\gamma$; the nucleus recoils with a momentum equal and opposite to that of the γ ray. Defining $\Delta E = E_i - E_f$ and using the relativistic relationship $E_\gamma = cp_\gamma$,

$$\Delta E = E_\gamma + \frac{E_\gamma^2}{2Mc^2} \quad (10.2)$$